PL-TR-94-2258

DESIGN, EVALUATION, AND CONSTRUCTION OF TEXESS AND LUXESS, AND RESEARCH IN MINI-ARRAY TECHNOLOGY AND USE OF DATA FROM SINGLE STATIONS AND SPARSE NETWORKS

Eugene Herrin
Paul Golden
Herbert Robertson

Southern Methodist University
Dallas, TX 75275

October 1994

Scientific Report No. 2

PHILLIPS LABORATORY
Directorate of Geophysics
AIR FORCE MATERIEL COMMAND
HANSCOM AFB, MA 01731-3010

SPONSORED BY
Advanced Research Projects Agency (DoD)
Nuclear Monitoring Research Office
ARPA ORDER NO A128

MONITORED BY
Phillips Laboratory
CONTRACT NO. F19628-93-C-0057

The views and conclusions contained in this document are those of the authors and should not be interpreted as representing the official policies, either express or implied, of the Air Force or the U.S. Government.

This technical report has been reviewed and is approved for publication.

JAMES F. LEWKOWICZ
Contract Manager
Earth Sciences Division

JAMES F. LEWKOWICZ, Director
Earth Sciences Division

This report has been reviewed by the ESC Public Affairs Office (PA) and is releasable to the National Technical Information Service (NTIS).

Qualified requestors may obtain additional copies from the Defense Technical Information Center. All others should apply to the National Technical Information Service.

If your address has changed, or if you wish to be removed from the mailing list, or if the addressee is no longer employed by your organization, please notify PL/TSI, 29 Randolph Road, Hanscom AFB, MA 01731-3010. This will assist us in maintaining a current mailing list.

Do not return copies of this report unless contractual obligations or notices on a specific document requires that it be returned.

REPORT DOCUMENTATION PAGE

Form Approved
OMB No. 0704-0188

1. AGENCY USE ONLY (Leave blank)	2. REPORT DATE	3. REPORT TYPE AND DATES COVERED
	October 1994	Scientific No. 2

4. TITLE AND SUBTITLE
Design, Evaluation & Construction of TEXESS and LUXESS and Research in Mini-Array Technology and Use of Data from Single Stations and Sprase Networks

5. FUNDING NUMBERS
PE 62301E
PR NM 93 TA GM WU AK
Contract F19628-93-C-0057

6. AUTHOR(S)
Eugene Herrin, Paul Golden, Herbert Robertson

7. PERFORMING ORGANIZATION NAME(S) AND ADDRESS(ES)
Southern Methodist University
Dallas, TX 75275

8. PERFORMING ORGANIZATION REPORT NUMBER

9. SPONSORING/MONITORING AGENCY NAME(S) AND ADDRESS(ES)
Phillips Laboratory
29 Randolph Road
Hanscom AFB, MA 01731-3010
Contract Manager: James Lewkowicz/GPEH

10. SPONSORING/MONITORING AGENCY REPORT NUMBER
PL-TR-94-2258

11. SUPPLEMENTARY NOTES

12a. DISTRIBUTION/AVAILABILITY STATEMENT
Approved for public release; Distribution unlimited

12b. DISTRIBUTION CODE

13. ABSTRACT *(Maximum 200 words)*

Objectives of the contract are twofold: (1) to conduct research in seismic mini-array technology & use of data from single stations & sparse networks, and (2) to design, evaluate and construct 2 mini-array, TEXESS(Texas Experimental Seismic System) in s.w. Texas and LUXESS (Luxor Experimental Seismic System), which is n.e. of Luxor, Egypt. These two tasks are dubbed CLIN 1 & CLIN 2. The proposed design was along the lines of a GSE Alpha Station. TEXESS was installed by SMU personnel the week of Aug 22, 1993, & the 1st event was a local, recorded on 31 Aug. With de-installation on hold until diplomatic agreements are in place between the U.S. and Egypt for the installation of LUXESS, work has been directed to CLIN 1 research; array processing, Ms:mb studies, & the AR (3) discrimination method.

Research on time-domain processing of array data has resulted in a significant decrease in the standard deviation of azimuths as compared with this statistic obtained using f-k processing. The Ms:mb method is an effective and transportable discriminant for shallow events with mb greater than 4.75. Autoregressive (AR) modeling on Lg data has resulted in the ability to discriminate small economic explosions from small earthquakes.

14. SUBJECT TERMS
Time-domain processing of array data Standard deviation of azimuths; f-k processing Ms:mb method; autoregressive (AR) modeling.

15. NUMBER OF PAGES
72

16. PRICE CODE

17. SECURITY CLASSIFICATION OF REPORT	18. SECURITY CLASSIFICATION OF THIS PAGE	19. SECURITY CLASSIFICATION OF ABSTRACT	20. LIMITATION OF ABSTRACT
unclassified	unclassified	unclassified	SAR

CONTENTS

ILLUSTRATIONS

Appendix 1.

Appendix 2.

ILLUSTRATIONS

ILLUSTRATIONS

TABLES

SUMMARY

Personnel contributing to this contract are: (1) Dr. Eugene Herrin, Principal Investigator, (2) Paul Golden, Project Director, (3) Karl Thomason, Chief Engineer, (4) Nancy Cunningham, Director - Computer Laboratory, (5) David Anderson, Systems Analyst, (6) Dyann Anderson, Administration, (7) Dick Arnett, Consultant, (8) Herbert Robertson, Consultant, (9) Jack Swanson, Consultant (10) Victoria L. Hammill, Consultant and (11) Billie Myers, Consultant. Ph. D. students include: (1) Chris Hayward, (2) Relu Burlacu, and (3) Zenglin Cui.

Objectives

Objectives of the contract are twofold: (1) to conduct research in seismic mini-array technology and use of data from single stations and sparse networks, and (2) to design, evaluate, and construct two mini-arrays, TEXESS (Texas Experimental Seismic System) in Southwest Texas and LUXESS (Luxor Experimental Seismic System), which is northeast of Luxor, Egypt. These two tasks are dubbed CLIN 1 and CLIN 2.

The original CLIN 1 objectives were to: (1) conduct research in the use of single station and sparse network data in detecting and identifying small seismic events, (2) conduct research to develop optimum configurations and processing techniques for a nine-element mini-array, and (3) to continue development of an unmanned intelligent seismic station. These objectives have been revised by the Project Office in April 1994 as described on page 6 under **Implications for Further Research**.

CLIN 2 objectives are to: (1) acquire hardware and software, (2) install TEXESS, (3) perform site surveys and choose location for LUXESS, (4) test TEXESS and perform verification tests prior to de-installation, (5) de-install TEXESS, (6) complete civil work in Egypt, (7) install and test LUXESS, (8) de-install data acquisition, analysis and archiving equipment and ship to Helwan, Egypt, data center, and (9) install and test data acquisition, analysis and archiving equipment at Helwan data center.

Technical Problem

The German Experimental Seismic System (GERESS) was dedicated in 1992 and represents an upgrade for regional arrays. Although GERESS was technologically advanced over NORESS and ARCESS, which were earlier regional arrays, because of greater sensitivity and wider dynamic range, there was a considerable effort that resulted in increased costs for pier and vault construction and trenching for power cabling. Now in TEXESS, there are innovations in emplacement techniques, which include the installation of sensors in shallow boreholes instead of vaults and the use of solar power at each site to eliminate cabling from a central-power source, that have reduced array-installation costs by an order of magnitude. TEXESS is, therefore, a proposed design for a GSE-Alpha station because of these cost-cutting innovations. In addition to design, construction, installation, and operation, of TEXESS, research will be undertaken to develop new means of taking data and handling the data.

General Methodology

In GSE/US/84, February 1993, entitled "Technical Concepts for an International Data Exchange System," the GSE established the design goals of a future system. Goals are:

1. Provide *prompt* access to all *essential* data,
2. Provide *convenient* access to all *available* data,
3. Provide direct access to all data at authorized national and global facilities, and
4. Accomplish goals with realistic manpower and budget resources.

The new concept of a global system for data exchange calls for an Alpha Network of 40-60 stations, primarily arrays; plus much greater than 60 Regional or Beta Stations; plus Local and National Networks or Gamma Stations.

SMU began research on mini-array technology in 1991 on a previous contract. The proposed design was along the lines of an Alpha Station consisting of an array containing nine sites. Advancements over the GERESS design included the following:

1. The placement of seismometers and electronics in boreholes to greatly reduce construction costs for piers and vaults
2. The use of solar power at each site rather than a central-power source
3. The use of GPS receivers for time data at each seismometer site to replace central timing from the Hub
4. The employment of radio links from seismometer sites to the Hub to replace cable links and associated construction costs
5. The use of modular equipment to facilitate the installation and maintenance of the array.

Four shallow boreholes about 7 meters deep and 11-5/8-in. in diameter were drilled and cased with standard 8-in. pipe. Special equipment and techniques were developed to lower and level seismometers in the boreholes. A prototype solar power array and directional antenna were also developed for installation at LTX.

Technical Results

The limited program described above was successful and SMU was granted on 26 April 1993 Contract No. F19628-93-C-0057 to design, evaluate, and construct two nine element experimental mini-arrays: TEXESS and LUXESS.

Important Findings and Conclusions

The SMU mini-array research program that was begun in 1991 under the previous contract proved the feasibility of the proposed design and methodology described above.

Significant Hardware Development

Preliminary research has led to the following hardware developments:

1. The development of seismometer emplacement techniques in boreholes, including remote seismometer locking eliminated the need for vaults
2. Advancements in computer applications and radio modems allow all necessary electronic components to fit inside a 8-in. casing to provide physical protection and a more stable environment for the electronics
3. The use of Global Positioning Satellite (GPS) receivers to obtain timing accurate to within 10 μs of world time assuring time synchronization of the array
4. The use of modern digital radio modems allows the system to perform as a local area network referred to as a RAN (Radio Area Network); radio polling software provides wide bandwidth intra-array communications while requiring two base-station radios; the need for expensive buried fiber-optic cable is eliminated
5. A NEMA enclosure is mounted on top of the borehole and is used to house the batteries and as a mount for the solar-power array; the GPS receiver and radio antenna are mounted above it.

Special Comments

The task of adapting the solar-panel arrays at Lajitas to the LUXOR environment is simplified somewhat in that both TEXESS and LUXESS are at approximately the same latitude, 30 deg North; both are in arid climatic zones; and both have about 3,500 annual hours of sunshine. As a result, there would be no need to modify the prototypic TEXESS design because of differing environmental conditions at LUXESS.

Implications for Further Research

CLIN 1 objectives were revised by the Project Office in April 1994 to: (1) conduct research to develop optimum configurations and processing techniques for a nine- and sixteen-element short-period arrays, (2) conduct research in discrimination of nuclear events using autoregressive (AR)

modeling techniques on Lg data, and (3) conduct research in measuring 20-second Rayleigh waves at regional distances using high-resolution, wide-dynamic-range, short-period, seismic-array data and broadband KS 36000 data.

CLIN 1 -- RESEARCH

Array Research

Conduct research to develop optimum configurations and processing techniques for nine-and-sixteen element short-period arrays,

In Scientific Report No. 1, PL-TR-94-2106, we discussed the problems of the large scatter of the order of ± 15 deg of azimuth estimates at GERESS after *f-k* processing. In order to address this problem, SMU research has concentrated on developing a time-domain processing techniques to reduce this statistic using the nine-element TEXESS array (see Figure 3, TEXESS Map, in cited report). The array-processing technique is similar to that described by Bernard Massinon in his paper entitled "The French seismic network -- current status and future prospects," which he presented at the GERESS Dedication and Symposium on 24 June 1992. The processing algorithm developed by SMU using GERESS D-ring data, which approximates the proposed 9-element TEXESS array, was presented in SMU-R-92-396, p. 14-17.

Appendix 1 is a report on array research.

Discrimination Research

Conduct research in discrimination of nuclear events using autoregressive (AR) modeling techniques on Lg data

In the framework of a Comprehensive Test Ban Treaty (CTBT), discrimination between low-yield or decoupled nuclear explosions, economic explosions and small shallow earthquakes using the characteristics of the seismic waves becomes very important. Some of the economic explosions are multiple-source events with a time and space pattern dependent upon the type of application. The superposition of the seismic motion in the time

domain leads to regular amplification and suppression of spectral power in the frequency domain. As, in general, single events (single explosions or earthquakes) do not exhibit spectral modulations, their presence can be used in the discrimination between single and multiple events. The aim of the present study is to develop a fast and robust method of discriminating between earthquakes and economic explosions based on differences observed in the spectral content of the regional waveforms. The method is based on the parametric estimation of the power-spectral density (PSD) using the autoregressive (AR) Burg algorithm of order 3, which provides a fast method to emphasize the spectral differences.

Appendix 2 is a report on this work.

Conduct M_S:m_b research by measuring 20-second Rayleigh waves at regional distances using high-resolution, wide-dynamic-range, short-period, seismic-array data and broadband KS 54000 data.

The M_S:m_b discriminant has been investigated by a number of researchers for both regional and teleseismic events and explosions. Bases for the discriminant are (1) that explosions emit more energy in the form of high-frequency body waves and (2) that earthquakes emit more energy in surface waves having low frequency radiation; therefore, an Ms:m_b plot displays a significant separation of the two populations. The problem with the method is that of identifying small explosions; that is, the problem boils down to seismograph sensitivity. With the installation of new high-dynamic-range seismographs at TEXESS, planned research includes the determination of Ms from small earthquakes at regional distances using the TEXESS array data recorded by short-period GS-13 seismometers and a posthole, long-period KS 54000 seismometer.

Victoria L. Hammill has begun development of discrimination software to provide an automated system of analysis for event discrimination through the development of public domain seismic applications software, with particular emphasis on conversion of cumbersome CALPLOT graphics to more efficient Matlab graphics.

Appendix 3 is a report on M_S:m_b research, and Appendix 4 is a Poster Session on discrimination research at SMU.

CLIN 2 -- DESIGN, EVALUATION, AND CONSTRUCTION OF TEXESS AND LUXESS

Experimental-Array Program

Information on the experimental-array program at SMU on the previous contract was presented in SMU-R-92-396 and in Scientific Report No. 1, PL-TR-94-2106 (ADA284580).

TEXESS AND LUXESS

Acquisition of Hardware and Software

The First and Second Quarterly R & D Status Reports cover the acquisition of hardware and software. TEXESS and LUXESS equipment is discussed in Scientific Report No. 1, PL-TR-94-2106. Instructions for the installation of the Posthole 54000 seismometer are presented in Appendix 5 of this report.

Array Hardware

Hardware is discussed in Scientific Report No. 1, PL-TR-94-2106.

Computer Hardware

Computer equipment is discussed in Scientific Report No. 1, PL-TR-94-2106.

Software

Acquisition of software was addressed in Scientific Report No. 1, PL-TR-94-2106.

Install TEXESS

Layout

TEXESS layout is discussed in Scientific Report No. 1, PL-TR-94-2106.

Installation

Installation is discussed in Scientific Report No. 1, PL-TR-94-2106.

Perform Site Surveys and Choose Locations for LUXESS

SMU has received communications from the National Research Institute of Astronomy and Geophysics (NRIAG), Helwan, Egypt, requesting a draft Memorandum of Understanding (MOU). Arrangements are presently being pursued by respective State Departments.

Test TEXESS Prior To De-installation

System fidelity tests were conducted by Chris Hayward and Dick Kromer during the week of 14 November 1993. During this period, engineering refinements were made by Karl Thomason.

De-install TEXESS

During the early part of the week of 21 November, SMU principals made an inspection trip to TEXESS in order to make plans for de-installation, packing, and international shipment.

APPENDIX 1. -- ARRAY-PROCESSING RESEARCH

A flow diagram for the array-processing algorithm is presented in Figure 1. After computing the cross-correlations of all channels relative to a reference channel and determining the indices of maximum correlation for each channel, relative time delays, Δt's, are computed. Using trial azimuths and incrementing by 1 degree, time residuals are computed and the rms residual is calculated for each azimuth. The process is repeated using each of the nine stations as reference channels. The trial azimuth yielding the minimum rms residual is selected as the *true* azimuth. Figure 2 shows the standard deviation, SD, of the *true* azimuth is 1.4 deg when using all nine channels as reference.

Having selected the best azimuth, one station is chosen as the reference channel and the time differences are corrected for elevation, using a trial replacement velocity. The differences are then regressed against the distances from the reference channel and the slope of the line gives the velocity, Vh, and the residuals for each station are then computed and regressed against the elevation differences determining the best replacement velocity, Vr, as shown in Figure 3. This procedure is then repeated using each station as the reference channel and the velocities, Vh and Vr, are averaged to yield the true velocities to aid in the determining the phase of the arrival as shown in Figure 4. Figure 5 shows standard deviations of azimuths of 7.1 obtained by *f-k* processing of the 25-element GERESS, which decreases to 5 deg using time-domain processing of 9-elements of the GERESS array to simulate the TEXESS geometry.

For the 9-element TEXESS, cross-correlation techniques in the time domain were used to determine relative time delays, Δt's, between array elements for an event. After obtaining the Δt's, an iterative procedure was used to determine the azimuth, station correction, and phase velocity for the event. Time-domain processing eliminates the dual problems of space aliasing and side lobes of the main beam that are inherent in frequency-domain processing.

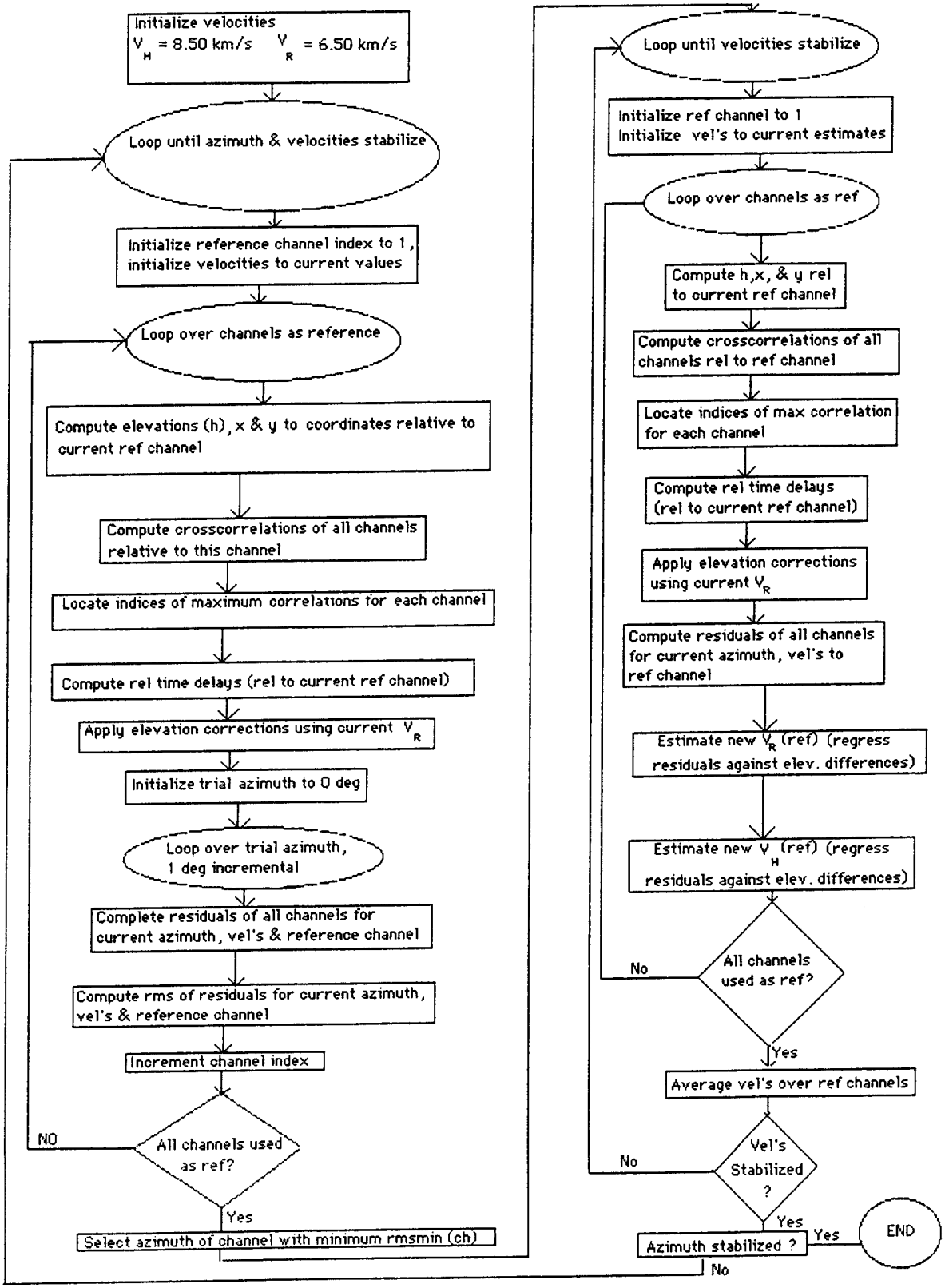

Figure 1. -- Flow Diagram of Time-domain, Array-processing Algorithm.

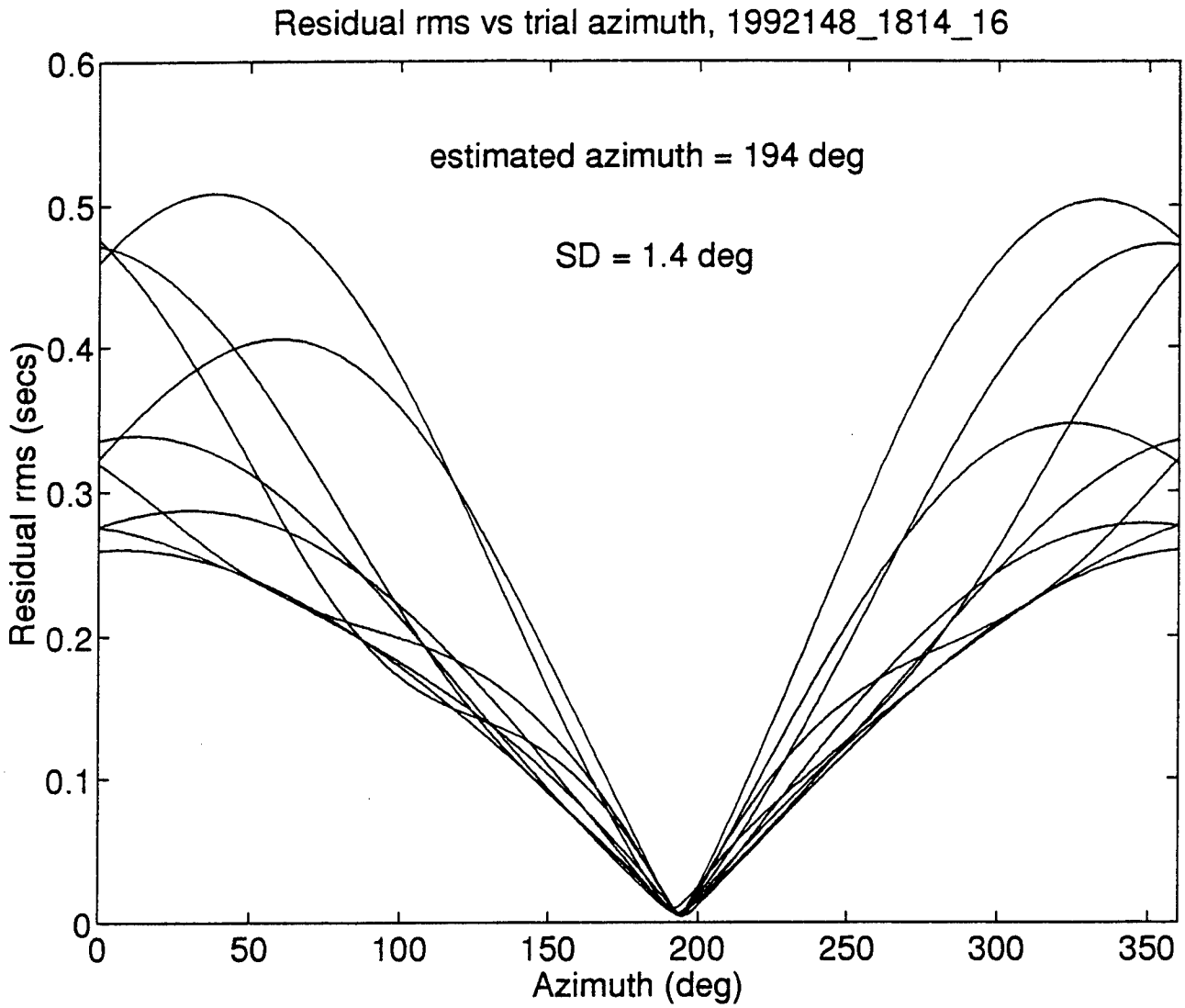

Figure 2. -- Trial Azimuth vs Residual rms Using 9-element GERESS D-ring.

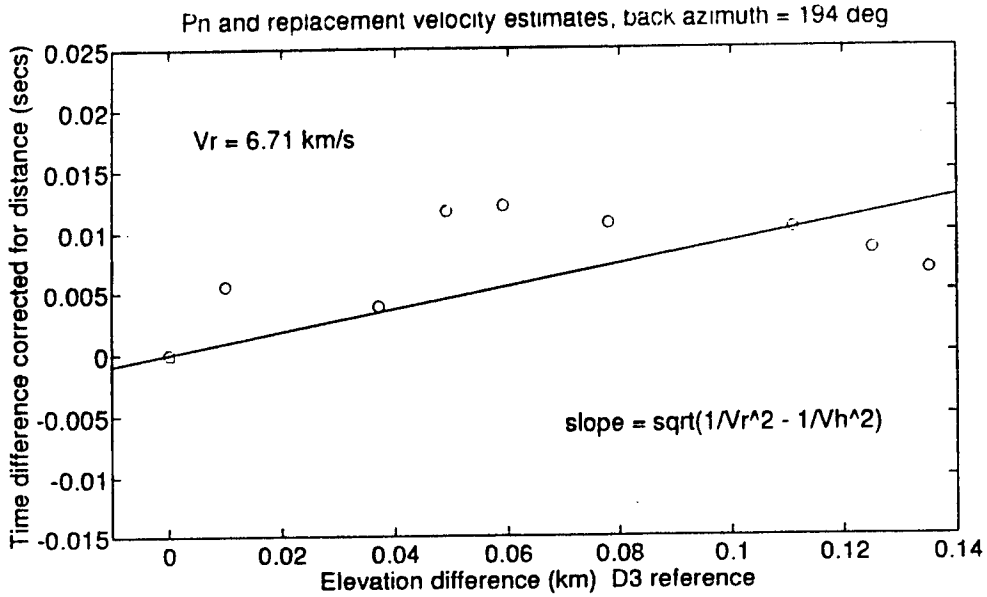

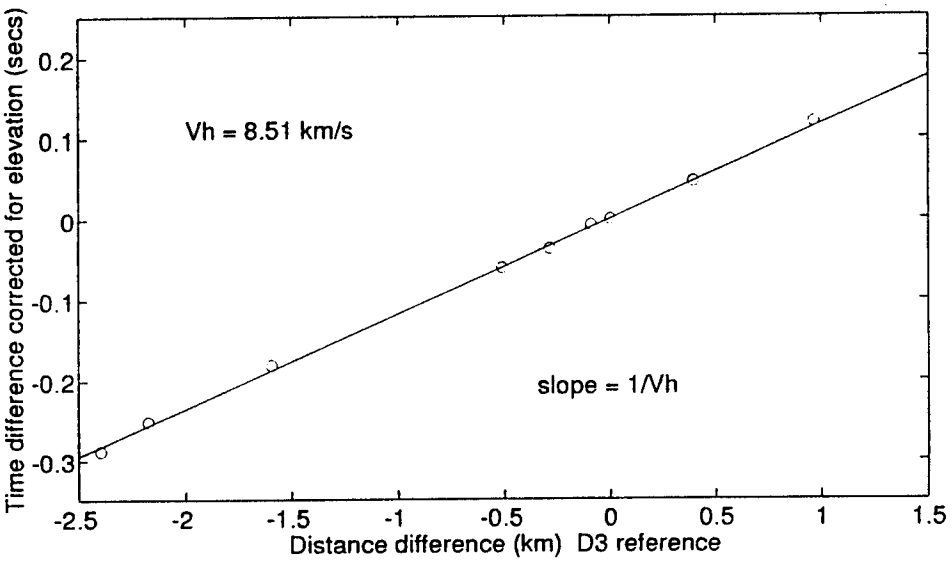

Figure 3. -- Regression Lines to Obtain Vh and Vr.

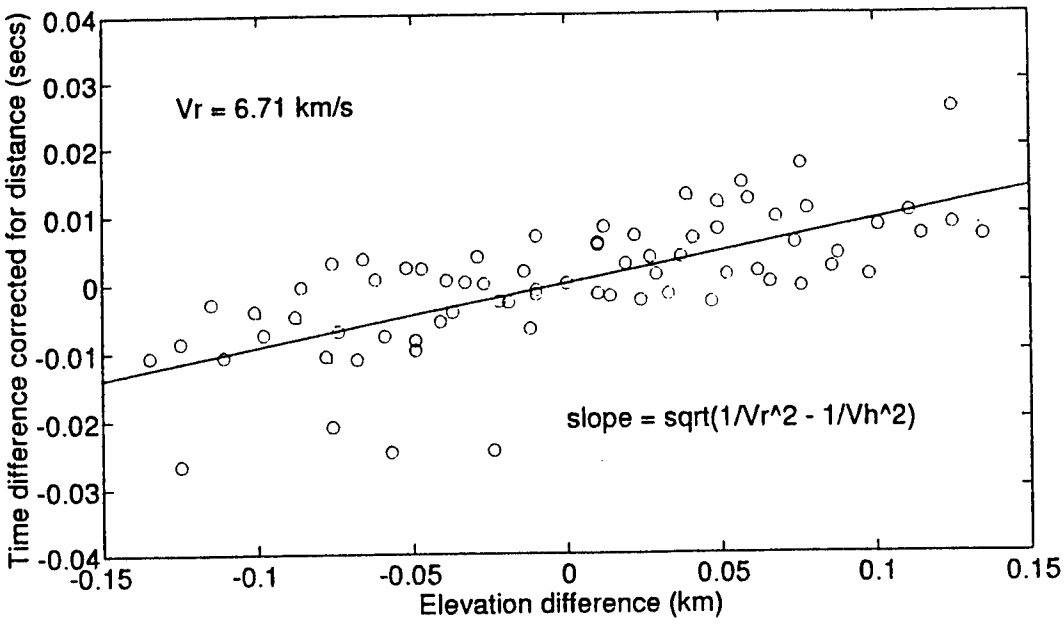

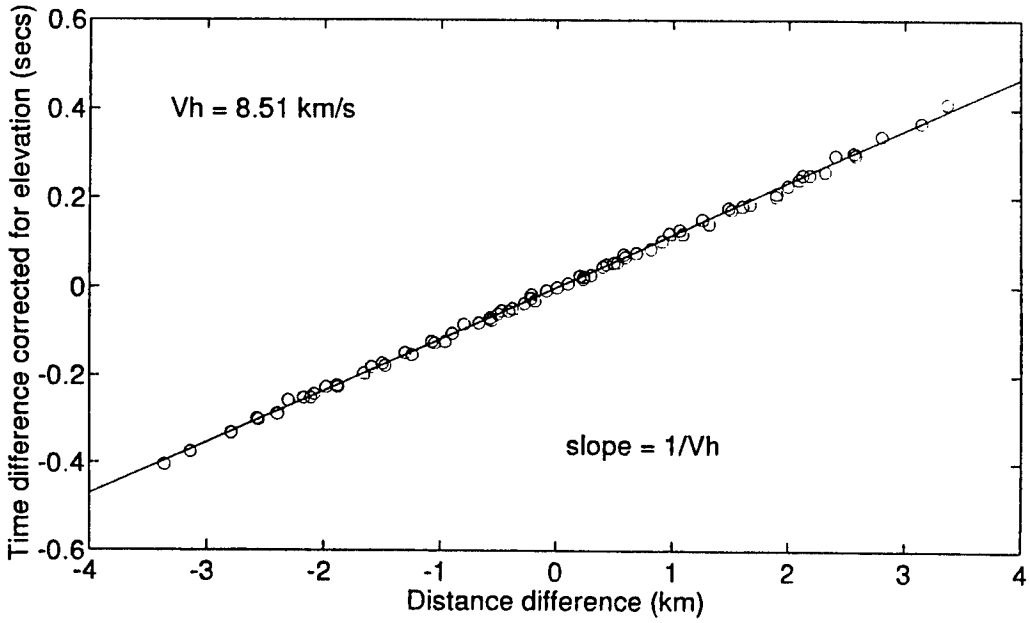

Figure 4. -- Regression Lines to Obtain *True* Vh and Vr.

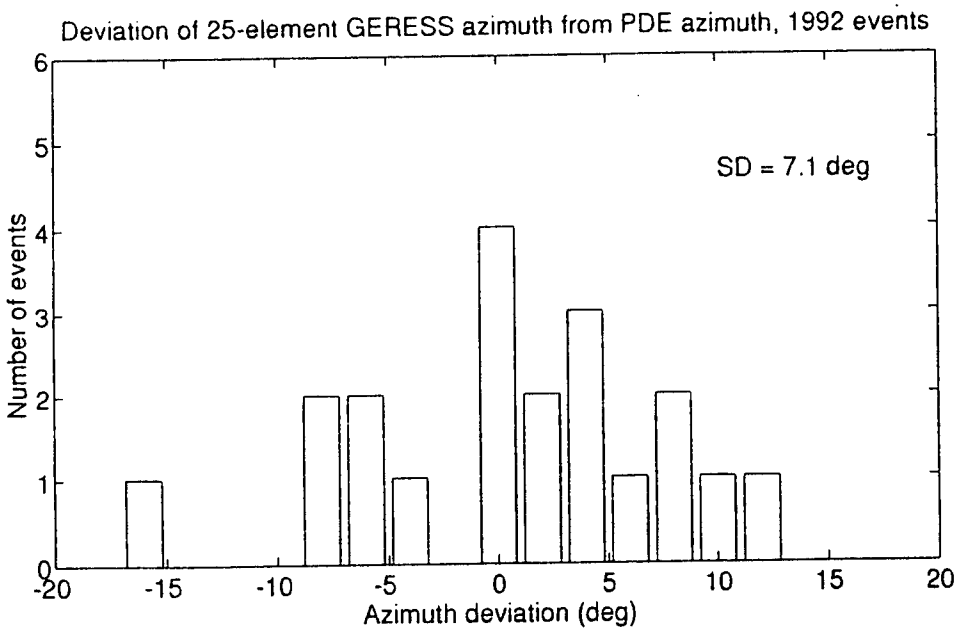

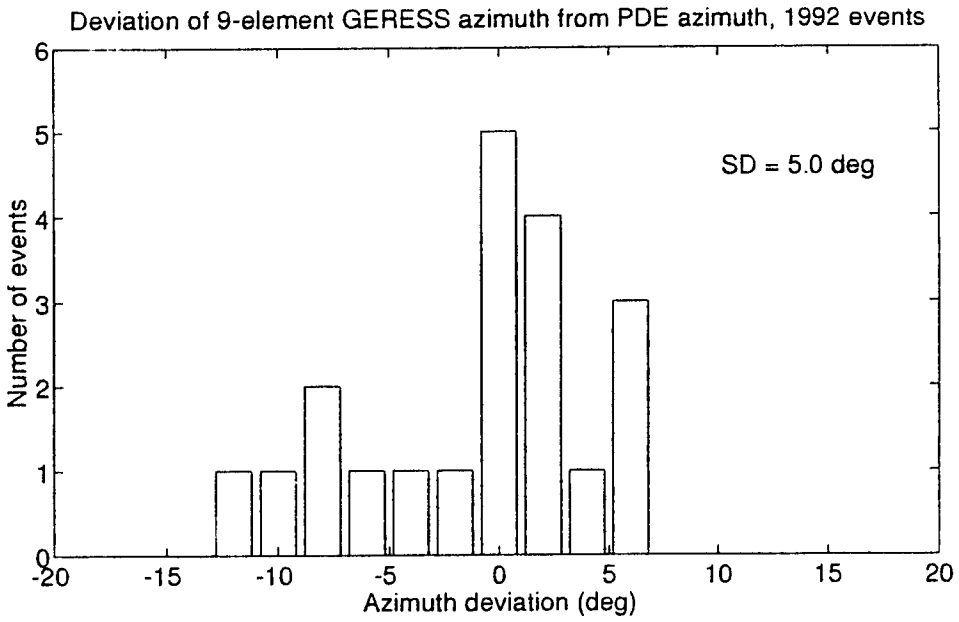

Figure 5. -- Histogram of Time Residuals Showing Decrease in Standard Deviation of Azimuths Using Time-domain Method Compared with *f-k* Method.

The following illustrations show the above technique applied to a magnitude 5.0 aftershock recorded by TEXESS on 19 January of the m_b=6.8 Northridge, California, earthquake of 17 January 1994. Figure 6 shows the P-wave arrivals bandpass filtered from 0.5 to 5.0 Hz. Time delays, Δt's, are computed from cross-correlations in a 2-sec-long time window. Figure 7 shows the rms error as a function of assumed azimuth for reference site, C1, using a P-wave velocity of 8.43 km/sec. The minimum rms error corresponds to an azimuth of 294°. Figure 8 shows the beam sum of the 8 vertical elements of the array with the beam steered at 294° using a velocity of 8.429 km/sec. Figure 9 shows the P-wave velocity determined by a least-squares fit to the residuals vs distance differences relative to the reference site, C1, using an azimuth of 294°. Figure 10 is the distribution of the time residuals using the same azimuth and a velocity of 8.43 km/sec.

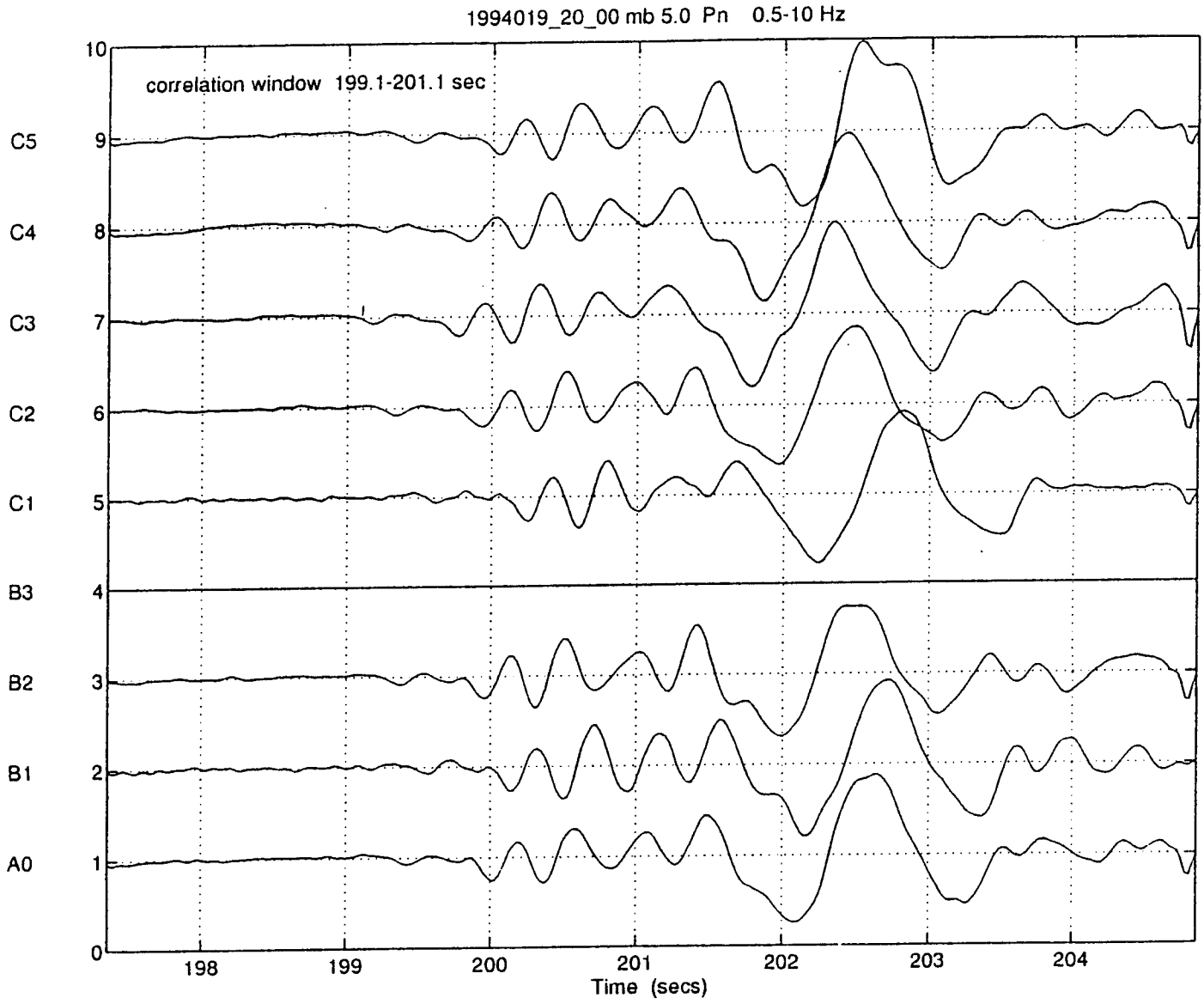

Figure 6. -- TEXESS P-wave Arrival for m_b=5 Northridge, CA, Aftershock of 19 January 1994 Following the Northridge m_b=6.8 Quake of 17 January 1994.

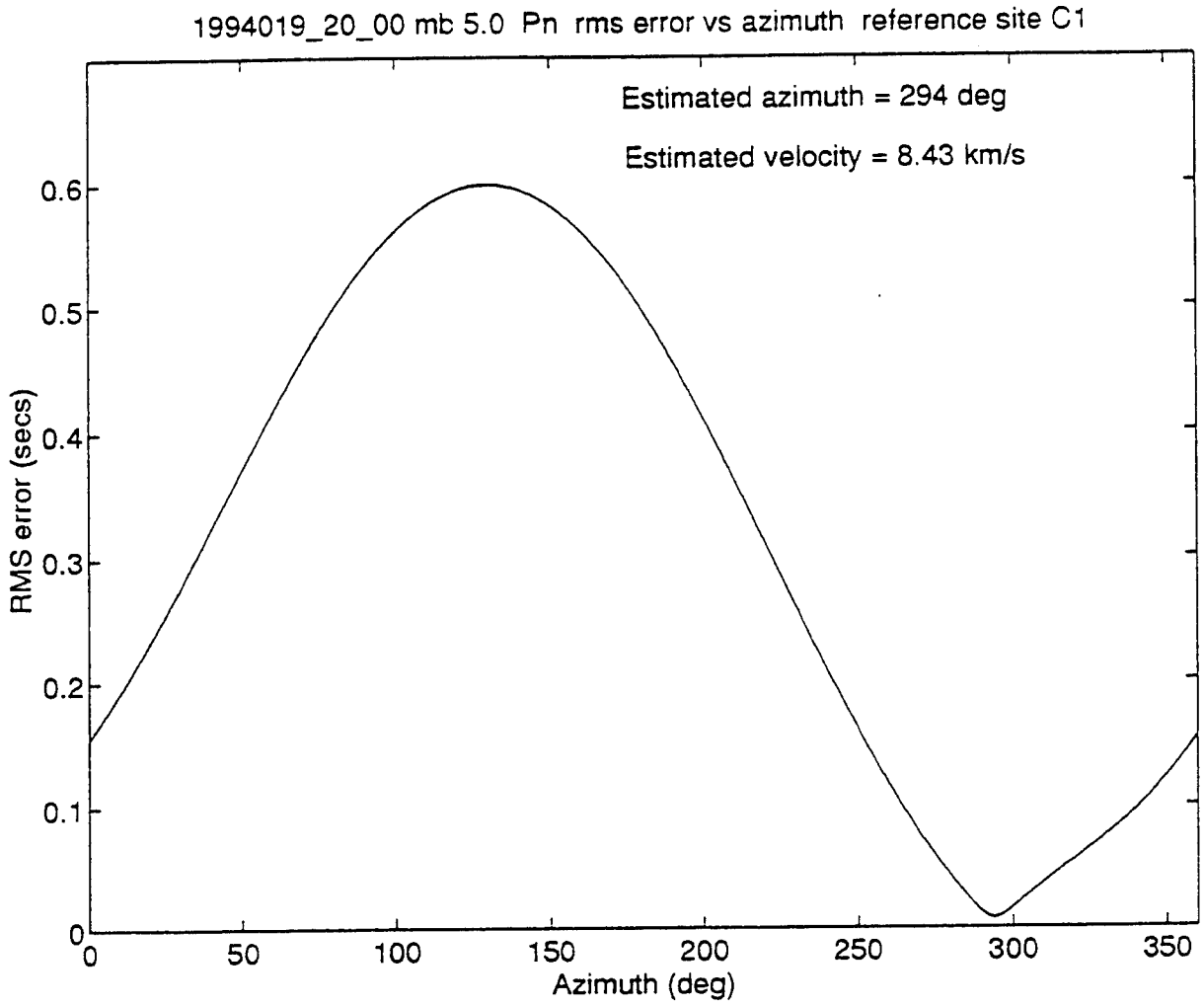

Figure 7. -- Azimuth vs rms Error.

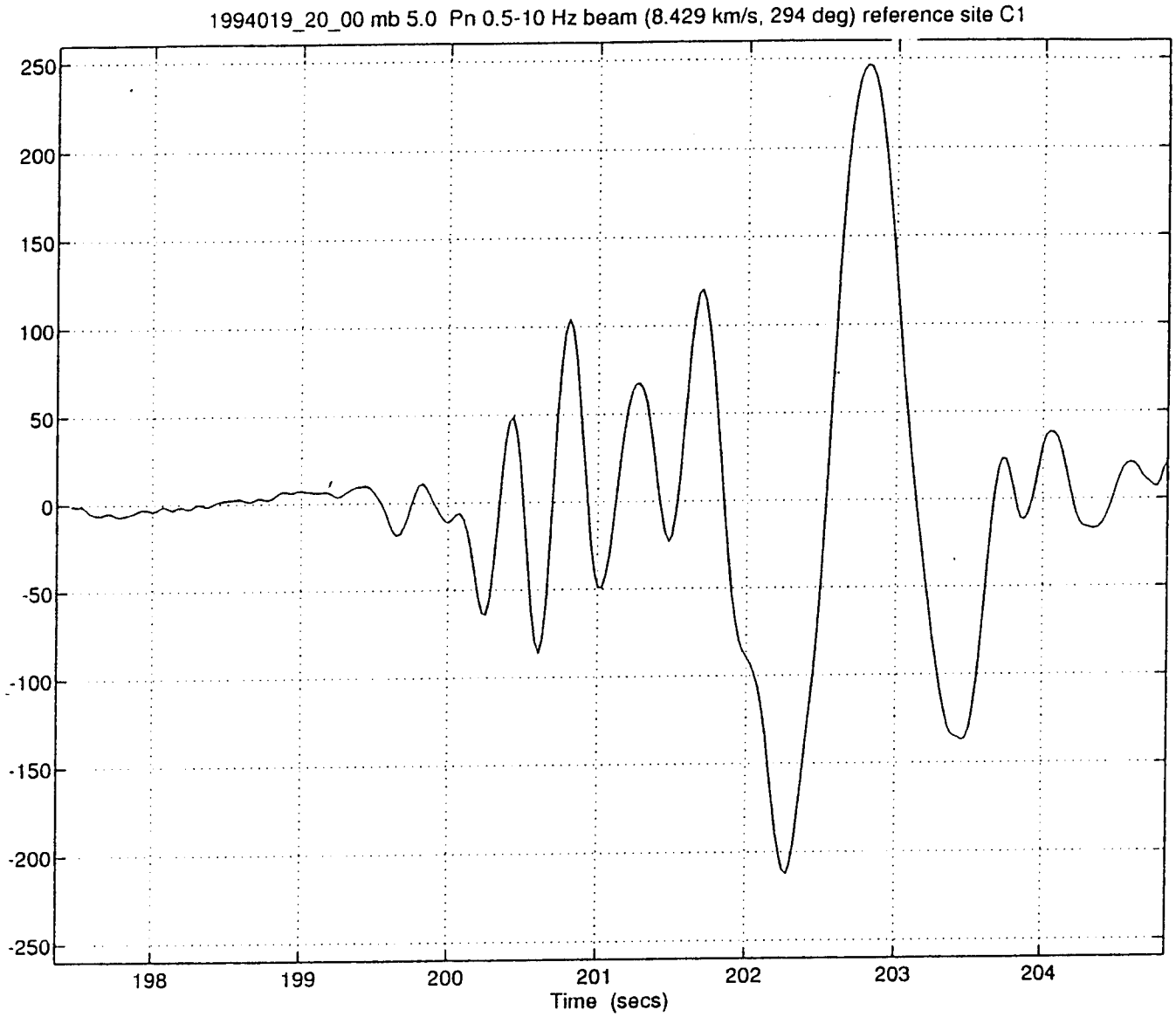

Figure 8. -- TEXESS Beam Sum.

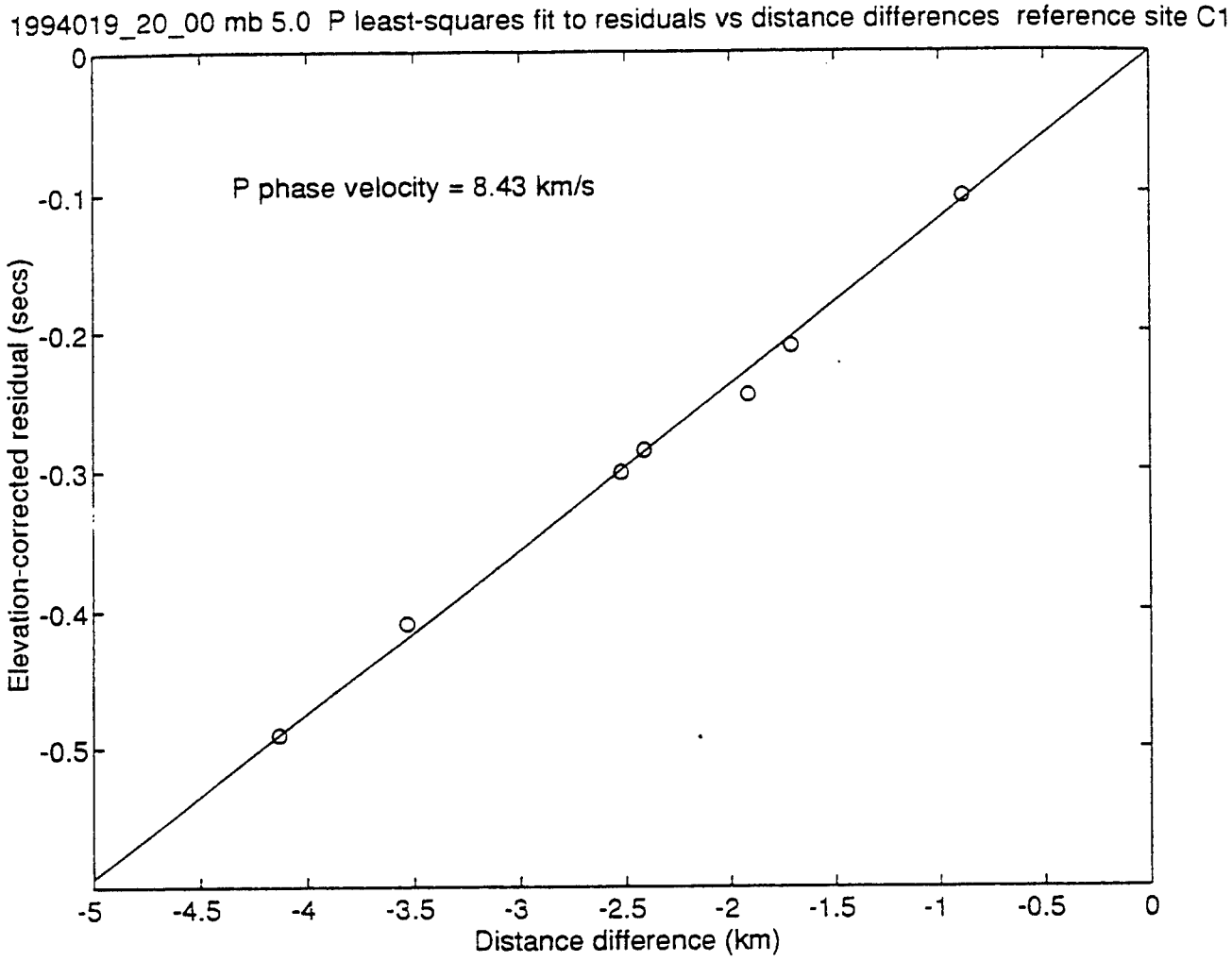

Figure 9. -- Distance Differences vs Residuals.

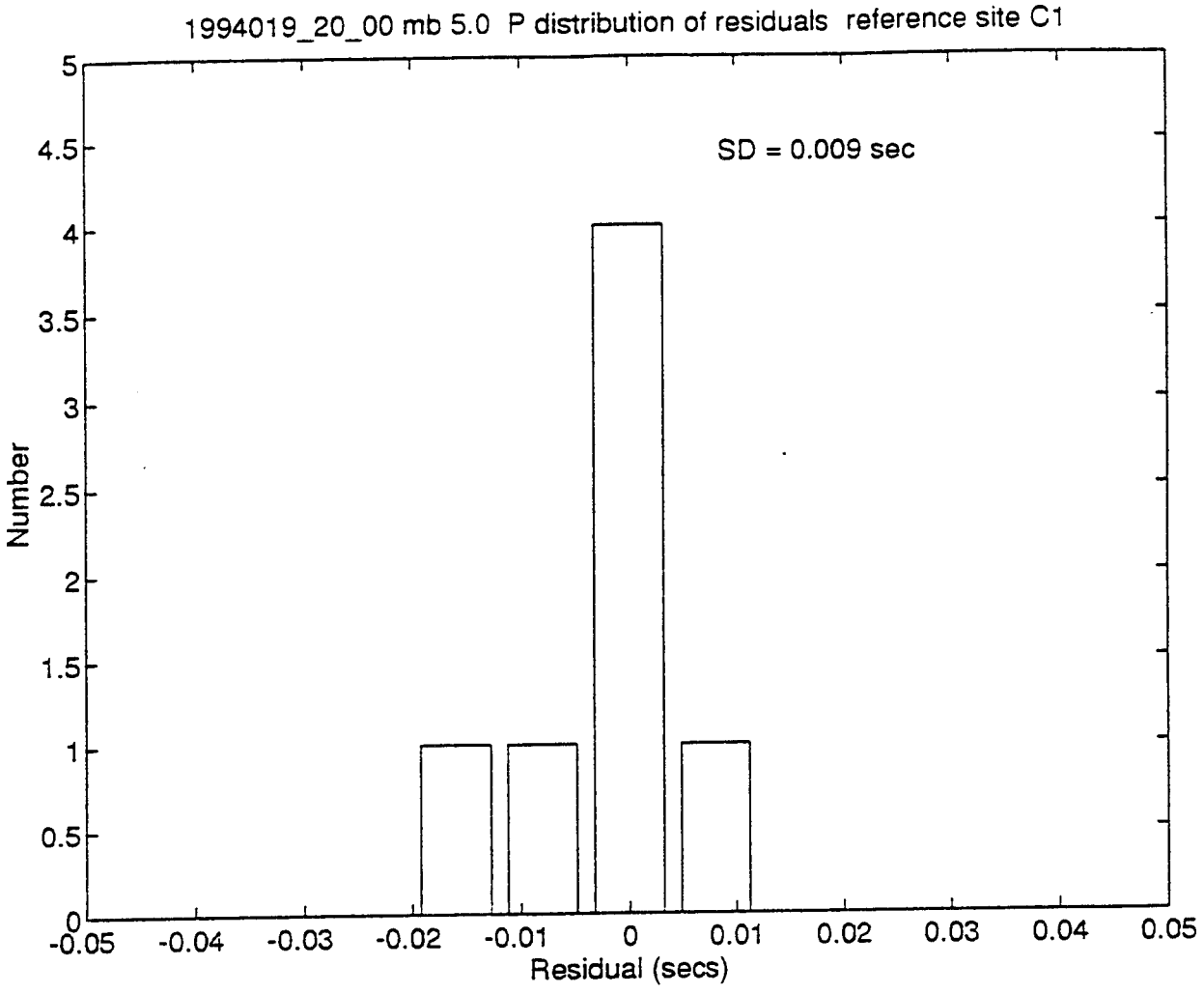

Figure 10. -- Histogram of Time Residuals.

APPENDIX 2. -- SPECTRAL DISCRIMINATION USING A PARAMETRIC APPROACH

Introduction

Spectral content of regional phases (Pn, Pg, Lg) has been shown to be important in the design of algorithms for discrimination between earthquakes and explosions (Murphy and Bennett, 1982). Techniques using spectral ratios have been applied to data in the Western U.S. and in Europe with reasonable success, but the transportability of the methods has not been satisfactorily established. Wüster (1993) used ARMA (Auto-Regressive, Moving Average) spectral estimates in the development of discriminants. All spectral discriminants based on regional arrivals have at this time at least two deficiencies:

(1) They have not been adequately tested against data with a variety of sources and propagation paths, and
(2) There is not an adequate explanation for why they work based on empirical or theoretical source models.

Research is underway to eliminate these deficiencies at least for one spectral discriminant that has been shown to work very well in central Europe.

Background

The discriminant we propose to study is based on autoregressive modeling of the Lg phase. The autoregressive spectral model is

$$x(n) = -\sum_{k=1}^{p} a(k)x(n-k) + u(n)$$

where p is the order of the process, a(k) are the coefficients and u(n) is the white noise driving process.

In the study discussed here AR order 3 was used. The resulting spectral model consists of one complex paired pole and one real pole, the latter being located at zero frequency for the events studied so far. (A real pole can only be

located at zero frequency or at the folding frequency.) The initial data is from the CSS Ground Truth Data Base (Grant et al., 1993) recorded at GERESS (16 Hz bandwidth). The data consists of explosions and earthquakes in the Vogtland area which are tabulated in Table 1. Figure 1 shows the third order autoregressive spectrum (AR(3)) for a quarry blast and Figure 2 shows the AR (3) spectrum for an earthquake. The frequency and reciprocal pole position of the complex pole in the AR (3) models were calculated using the Lg arrival for the events in Table 1. A value of 1.0 indicates that the reciprocal pole is on the unit circle, 0.0 indicates a position at the origin. Neither a value of 0.0 or 1.0 can occur in practice. Figure 3 shows reciprocal pole position versus frequency for the analyzed events. Solid circles are explosions and stars are earthquakes. The two open circles represent surface and buried explosions at the Tyrnyaus mine in the Caucasus Mountains of Southern Russia (Stump et al., 1994) recorded at station GUM. This figure shows a clear separation of explosions and earthquakes with the latter having broad AR(3) spectra with "weak" poles above 6 Hz while the explosions all show much "stronger" poles at frequencies less than 5 Hz. After reviewing the results shown in Figure 3, David Russell of AFTAC made the following comment (electronic communication, 1994):

> I must tell you I am very impressed with this approach, since:
> (1) It appears to work
> (2) It is robust, simple and straightforward (music to our ears here)
> (3) Last but certainly not least; it does not require extensive precalibration,
> such as taking out Q effects, etc.

Unresolved Technical Issues

The Lg discriminant based on a third order autoregressive model has been successfully applied to the available seismic data with a bandwidth of at least 15 Hz., where the nature of the source was clearly identified. Technical issues that now must be resolved can be simply described as follows:

(1) Will the method work for sources in other areas, particularly areas analogous to and within the Middle East?

Table 1. Earthquakes and Explosions From Vogtland Area

Event #	Date	Lat(N)	Long(E)	Depth	M	Yield(kg)	Origin time	Eq/Qb
1	3/11/91	50.207	12.685	0	1.98	3,265	12:03:23.986	qb
2	3/21/91	50.207	12.685	0	2.05	3,982	12:04:14.701	qb
3	3/22/91	50.207	12.685	0	2.03	2,835	12:33:25.332	qb
4	3/23/91	50.207	12.685	0	1.99	2,025	12:00:55.800	qb
5	3/24/91	50.296	12.225	12.9	2.18		05:05:04.447	eq
6	3/24/91	50.279	12.228	12.9	1.5		05:35:21.047	eq
7	3/24/91	50.277	12.24	13.9	1.4		06:57:59.309	eq
8	3/24/91	50.278	12.22	12.4	1.65		09:38:33.436	eq
9	3/24/91	50.294	12.223	12.7	2.07		14:33:27.988	eq
10	3/24/91	50.293	12.224	12.5	1.8		15:00:44.532	eq
11	3/24/91	50.293	12.224	9	1.73		15:41:03.515	eq
12	3/25/91	50.298	12.222	12.9	2.37		14:54:13.507	eq
13	3/25/91	50.292	12.213	12.4	1.54		22:31:45.761	eq
15	5/2/91	50.207	12.713	0	1.93	3,575	11:06:10.221	qb
16	5/2/91	50.184	12.186	0	2.03		12:47:33.067	qb
18	5/10/91	50.79	12.07	-999	1.43		20:02:51.112	eq
19	5/19/91	50.36	12.371	0	2.06		03:22:10.0	eq
20	5/23/91	50.207	12.713	0	2.12	3,135	11:01:05.259	qb
21	5/25/91	50.207	12.713	0	2.13	3,135	11:01:28.688	qb
22	5/26/91	50.207	12.713	0	2.14	2,907	11:00:32.367	qb
23	5/28/91	50.207	12.685	0	2.01	3,575	11:03:51.425	qb
24	6/20/91	50.207	12.685	0	1.98	1,998	11:01:16.808	qb
25	6/20/91	50.293	12.803	0	1.8		11:45;35.486	qb
26	6/22/91	50.207	12.685	0	2.15	2,886	10:58:34.818	qb
27	6/27/91	50.207	12.685	0	1.93	3,515	11:04:39.629	qb

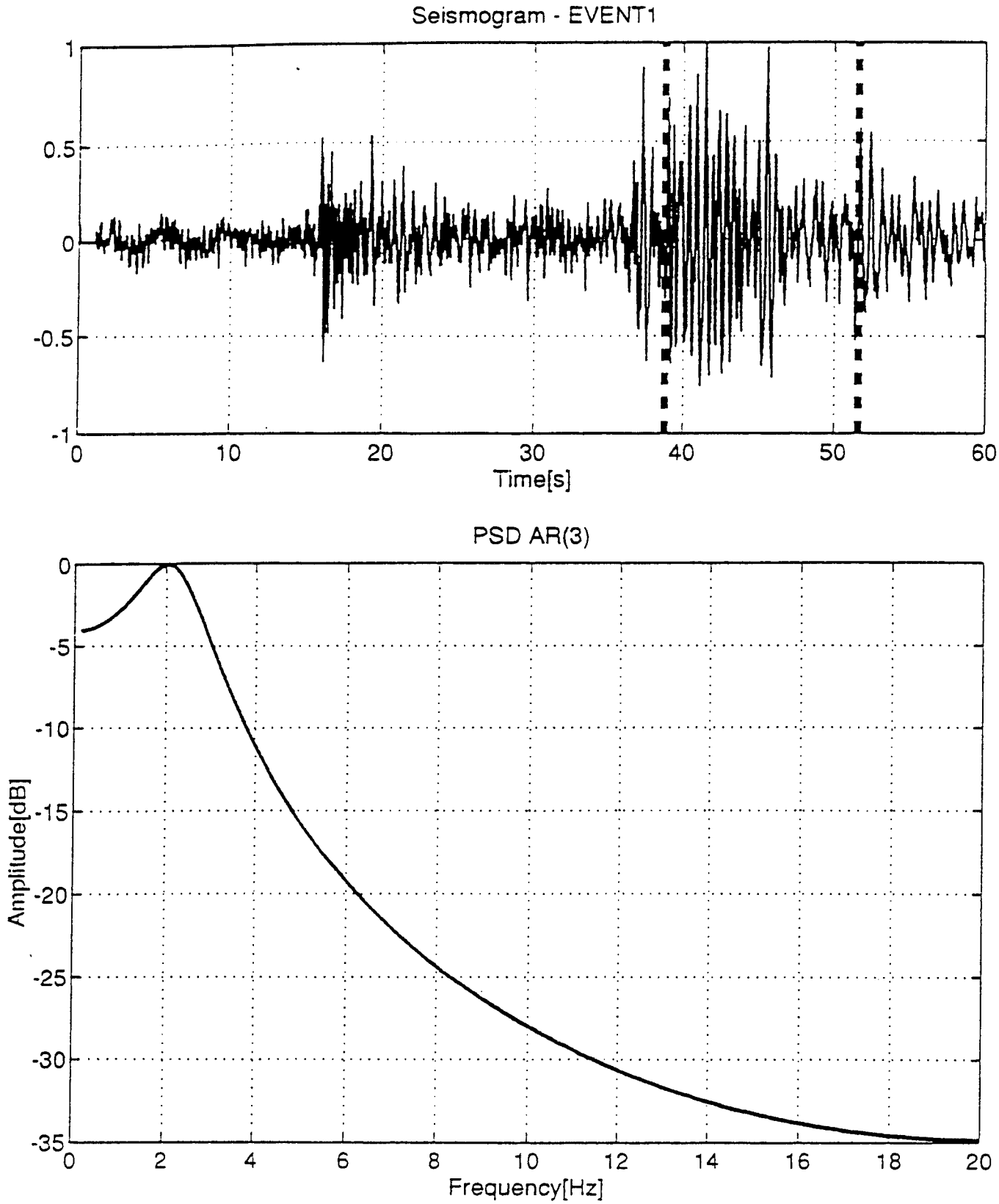

Figure 1. -- Seismogram and PSD AR(3) for EVENT 1.

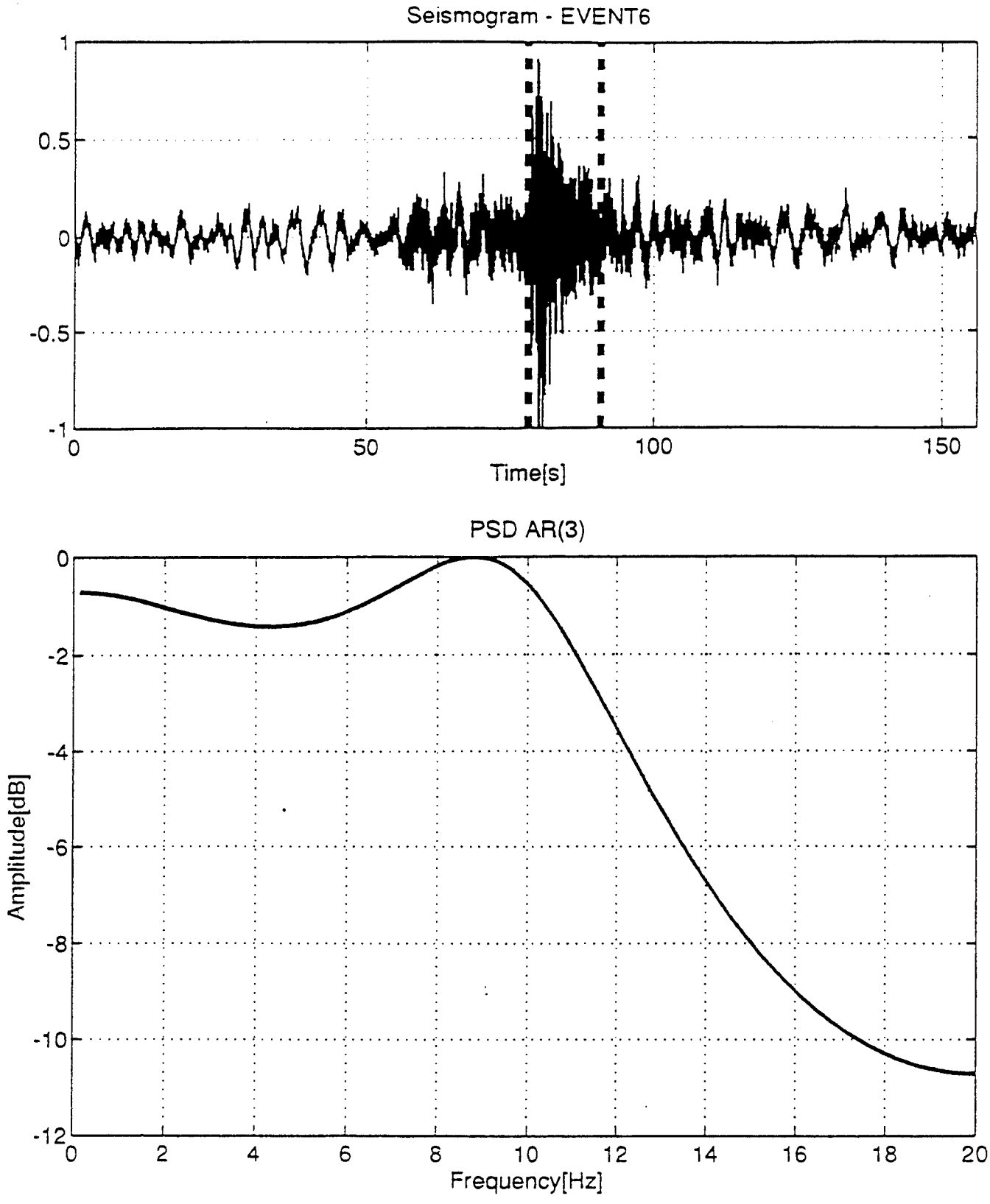

Figure 2. -- Seismogram and PSD AR(3) for EVENT 6.

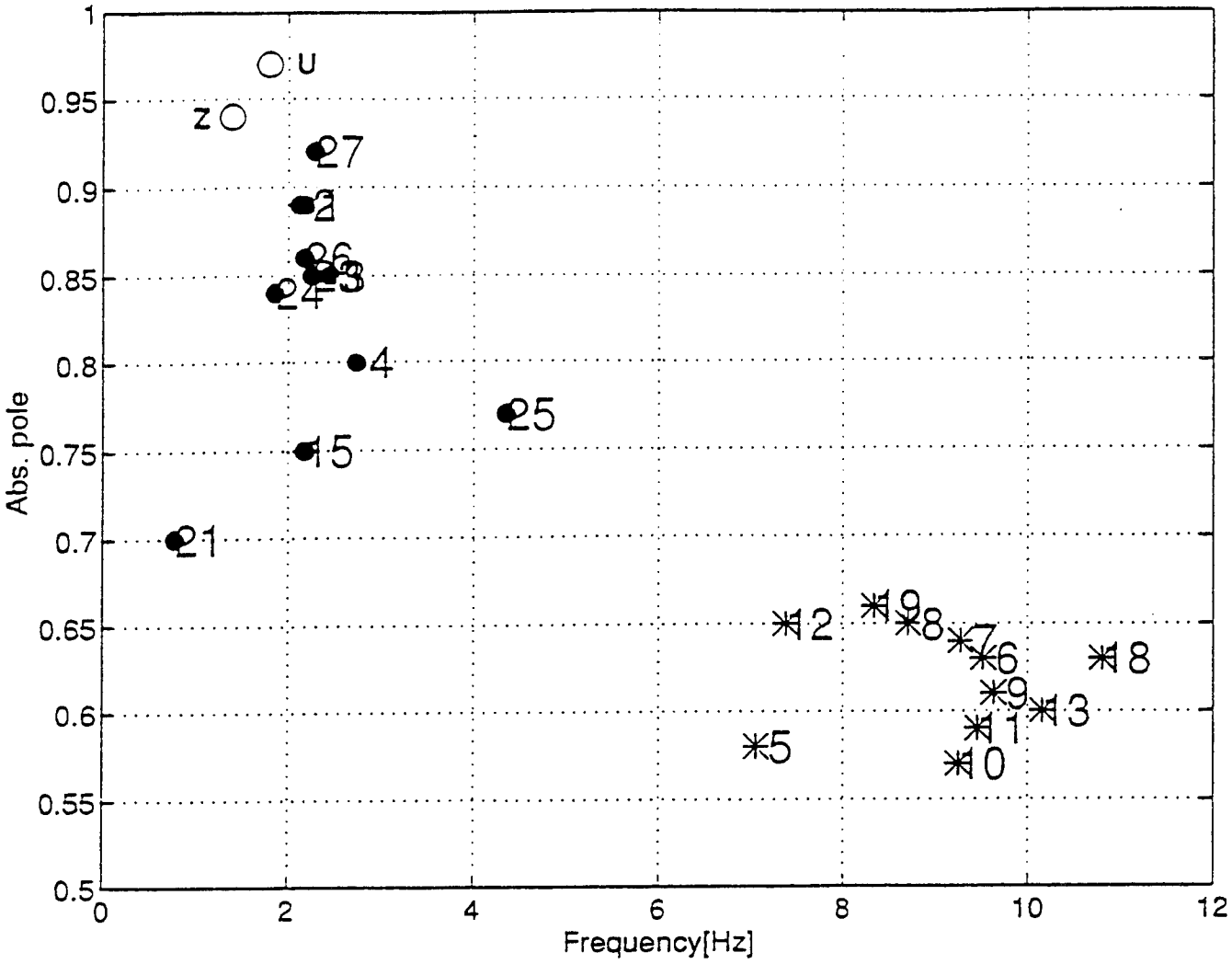

Figure 3. -- Absolute Pole Position as a Function of Frequency.

(2) The method has been tested only for events with ML around 2. Will the discriminant work equally well for larger events?

(3) Why does the method work at all? That is, why does the vertical component of the Lg signals recorded on systems having a flat velocity response from about 1 to 15 Hz show an apparent "corner frequency" of less than 5 Hz for shallow distributed explosions and greater than 6 Hz for earthquakes?

REFERENCES

Bou-Rabee, P., and P. Talwani, 1993, Was the magnitude 4.7 earthquake of June 2, 1993 near Burgan oil field, Kuwait induced?: *EOS Trans. AGU (Abstract)*

Davis, Scott D., Wayne D. Pennington and Steven M. Carlson,1989, A compendium of earthquakes in Texas:*Texas Bur. Econ. Geol. ,Geol. Circ.* 89-3, 89 p.

Davies, David (Rapporteur), 1968, Seismic Methods for Monitoring Underground Explosions: *SIPRI*, Stockholm, 130 p.

Doser, Diane I., Mark Baker and David Mason,1991, Seismicity in the War-Wink gas field, Delaware basin, west Texas and its relation to petroleum production:*Bull. Seis. Soc. Am.*, **81**, 971-986.

Grant, L., J. Coyne, and F. Ryall,1993, CSS Ground Truth Database: Version 1 Handbook: *Scientific Report*, C93-05, Center for Seismic Studies.

Grasso, J. R. and G. Wittlinger, 1990, Ten years of seismic monitoring over a gas field. *Bull. Seis. Soc. Am.*, **80**, 450-473.

Herrin, Eugene, and Tom Goforth,1977, Phase-matched Filters: Application to the study of Rayleigh waves: *Bull. Seis. Soc. Am.*, **67,** 1250-1275.

Keller, G.R., A. M. Rodgers and C.D. Orr,1987, Seismic activity in the Permian Basin area of west Texas and southeastern New Mexico: *Seis. Res. Ltrs.*, **58,** 63-70.

Muller, G.,1985, The reflectivity method: a tutorial: *J. Geophys.*, **58,** 153-174.

Murphy, J.R., and T.J. Bennett,1982, A discrimination analysis of short-period regional seismic data recorded at Tonto Forest Observatory, *Bull. Seism. Soc. Am.*, **72,** 1351-1366.

Peterson, Jon,1993, U.S. Geological Survey Open-File Report 92-322.

Raleigh, C.B., J.H. Healy and J. D. Bredehoft,1976, An experiment in earthquake control at Rangely Colorado: *Science,* **191,** 1230-1237.

Rodgers, Peter W., 1992, Frequency limits for seismometers as determined from Signal-to-Noise Ratios: Part 1. The Electromagnetic Seismometer: *Bull. Seis. Soc. Am.*, **82,** 1071-1098.

Stump, B.W., F. Riviere, I. Cernoby, and K. Koch,1994, Monitoring a test ban treaty presents scientific challenges: *EOS* , **75** (24) p,265

Wüster, J.,(1993, Discrimination of chemical explosions and earthquakes in central Europe - a case study: *Bull. Seis. Soc. Am.*, **83**, 1184-1212.

APPENDIX 3. -- DETERMINATION OF MS FROM REGIONAL EVENTS

Introduction

By 1970, research in the seismic discrimination of explosions and earthquakes had clearly established that the comparison of surface wave magnitude (Ms) and body wave magnitude (m_b) could be used to classify shallow events. In fact, this method provided the only reliable means for the seismic identification of underground explosions. The Ms:m_b method was shown to be an effective and transportable discriminant for shallow events with m_b greater than 4.75 (Davies, 1968). Further research was carried out including the construction of long-period arrays in an attempt to lower this threshold, but until recently, essentially all data was obtained from stations at teleseismic distances.

Now the construction of regional arrays for monitoring a proposed CTBT has led to considerable interest in reducing the detection threshold for fundamental mode Rayleigh waves using regional signals. The goal of our proposed studies is to identify shallow earthquakes at regional distances with magnitude (m_b) as low as 3.0 using the Ms:m_b method.

Previous Work

The GERESS regional array in eastern Bavaria provided the first high-resolution array data with linear dynamic range greater than 120 dB. Although in 1992 there was no broadband sensor at GERESS which could resolve long-period noise at a 20 sec. period, it was possible to use the short-period sensors for this purpose. The GS-13 sensors at GERESS have their resolution at 0.05 Hz (20 sec. period) limited by self-noise which is about 20 dB above the Low Noise Model (Peterson, 1993, and Rodgers, 1992). The random nature of this self-noise and the small aperture of the array relative to the wavelength of 20 sec. Rayleigh waves make it possible to improve the signal-to-noise ratio by about 14 dB simply by summing the output of the 25 short-period sensors. The 120 dB resolution then allows the sum to be low-pass filtered (corner at 0.1 Hz) in order to observe long-period signals. This method

has been used to resolve the ambient seismic background noise at GERESS at periods of 10 to 20 seconds.

The prototype ARPA Model 94 regional array at Lajitas (TEXESS) has nine vertical GS-13 (SP) elements and a post-hole KS36000 broadband (BB) system. The SP and BB data are recorded with linear dynamic range greater than 120 dB, with the SP's using SHI AIM 24 ADC's and the BB using an RDAS 200 ADC. The prototype post-hole KS36000 at TEXESS is sandpacked in a 7 m deep borehole resulting in a total installed cost less than half that of the standard KS36000 in a 100 m deep borehole. An AFTAC standard KS36000 system is collocated with the post-hole KS36000, but the data from that instrument are recorded with a linear dynamic range of about 70 to 80 dB.

The sum of the GS-13 elements at TEXESS results in a self-noise threshold about 10 dB above the Low Noise Model at a period of 20 sec. The posthole KS should be capable of resolving the Low Noise level at 20 sec. We have used both the SP array sum and the posthole BB vertical to look for 20 sec. Rayleigh waves in regional signals.

Aftershocks from the Northridge earthquake, a distance just over 1500 km from Lajitas, were used to prepare a database for which location, origin time, local magnitude and, in some cases, m_b were known from USGS reports. One aftershock on 19 January 1994 (m_b 5.0) was selected as a reference event. First the SP array was beamed at the event using a cross-correlation method to determine back azimuth, horizontal phase velocity and static corrections for the Pn arrival (az. 291°, vel. 8.46 km/sec.). Figure 1 shows that the residuals for this fit for all possible cross-correlations between elements are all less than one sample point (0.025 sec. for 40 sps data). The set of delays from this fit was used to form beams for 24 smaller aftershocks. These array sums were then used to compute m_b (Pn) for Lajitas, which are shown in the eighth column of Table 1.

Both the sum of the SP channels and the vertical BB (post-hole) channel were Butterworth, low-pass filtered at 0.10 Hz with three poles forward and three reversed in order to eliminate any phase shift. The filtered wave forms for the SP sum and BB Z were essentially identical. Figure 2 shows the results of

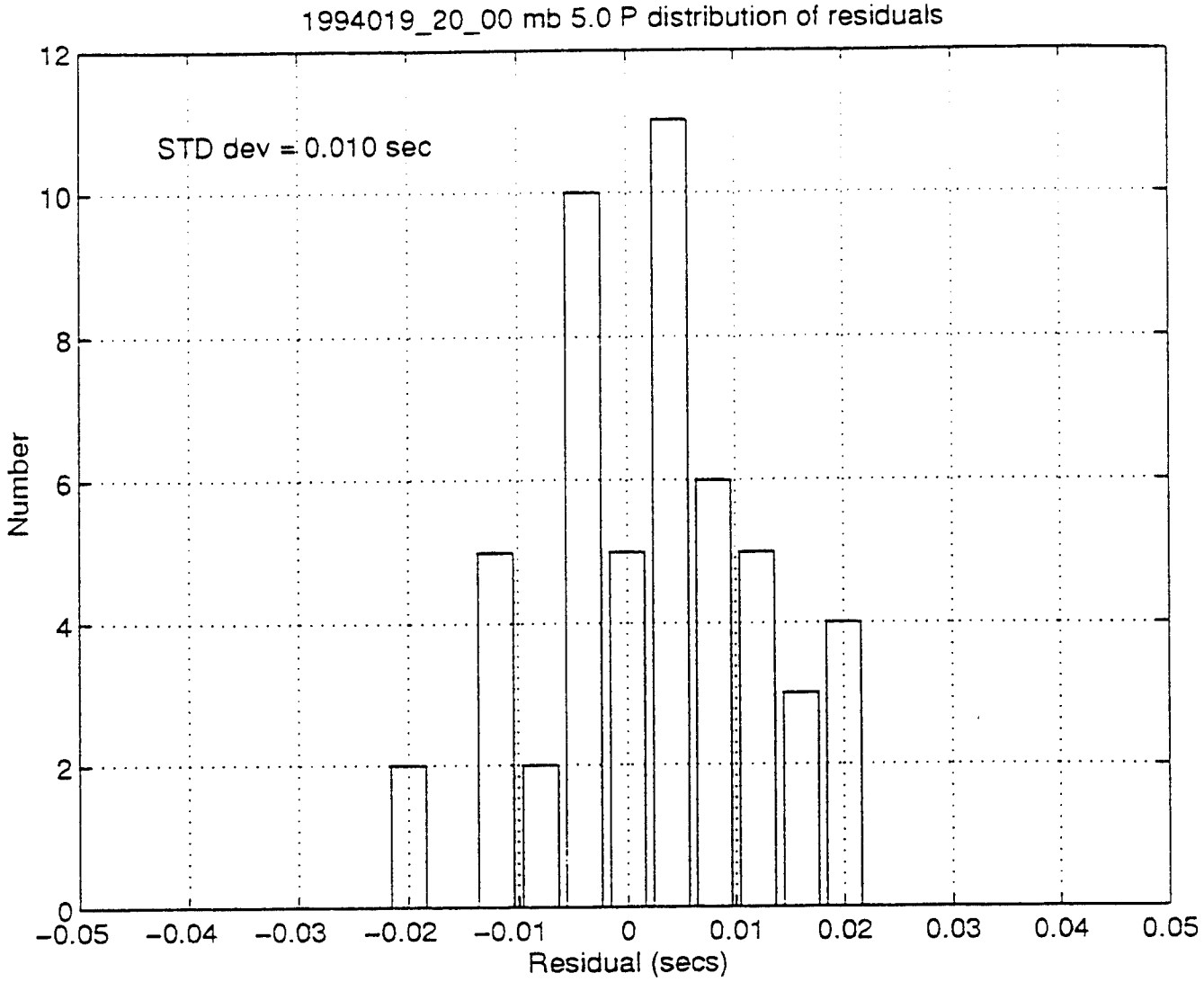

Histogram of residuals from least-squares estimate of azimuth and phase velocity of reference event 1994019_20_00 (aftershock of the Northridge earthquake) observed on the Lajitas, TX short period array. Data are combined for residuals obtained using each channel as reference. Estimated azimuth was 291 degrees and estimated phase velocity was 8.46km/s.

Figure 1. -- Histogram of Residuals from Northridge Aftershock.

Table 1. Selected Aftershocks of Northridge Earthquake of 17 January 1994

Event Identification	dy/mo/yr	Time (GMT)	Reported mb	Reported ML	Dist (km)	Azimuth (degrees)	P-wave (pn) magnitude (mb)	Surface-wave (sp) magnitude (LR)	Surface-wave (bb) magnitude (LR)
Reference Event-									
sig94019_20_00	19Jan94	21:09:26.4	5.0	5.3	1534.2	106.6	5.23	5.31	5.34
sig94029_08_00	29Jan94	11:20:35.9	4.5	5.0	1513.4	107.3	4.59	5.39	
sig94019_20_01	19Jan94	21:11:43.1	4.6	4.8	1521.7	106.9	4.43	4.90	4.85
sig94024_04_00	24Jan94	04:15:18.8	4.4	4.7	1512.4	107.5	4.33	3.76	
sig94019_12_00	19Jan94	14:09:11.9	4.3	4.5	1512.4	106.3	4.24	4.07	4.07
sig94019_04_00	19Jan94	04:40:46.1	4.1	4.5	1518.0	106.8	4.07	3.89	
sig94024_04_02	24Jan94	05:54:21.0	4.1	4.4	1519.6	107.4	4.14	3.66	
sig94024_04_01	24Jan94	05:50:24.3	4.2	4.3	1519.6	107.4	4.23	3.81	
sig94019_08_01	19Jan94	09:13:08.6		4.2	1531.8	106.5	4.18	3.16	3.23
sig94019_04_01	19Jan94	04:43:12.4		4.1	1531.3	106.7	4.24	3.61	3.62
sig94019_12_01	19Jan94	14:49:13.0		4.1	1505.5	106.9	4.04	3.51	3.47
sig94019_04_04	19Jan94	07:14:04.0		3.9	1507.6	106.8	4.02	3.27	
sig94032_04_01	1Feb94	07:40:19.1		3.8	1521.6	106.8	3.60	3.00	
sig94019_12_02	19Jan94	15:03:46.6		3.7	1502.1	107.2	3.60		
sig94019_16_02	19Jan94	19:50:07.8	3.3	3.7	1503.8	107.1	3.37		
sig94019_04_02	19Jan94	05:14:57.3		3.6	1502.7	107.0	3.39		
sig94019_20_02	19Jan94	21:27:50.2		3.5	1528.0	107.1	3.71		
sig94019_04_03	19Jan94	06:23:41.1		3.5	1501.1	107.3	3.16		
sig94032_08_00	1Feb94	09:59:10.1		3.4	1524.1	107.1	3.16		
sig94031_04_00	31Jan94	04:55:50.2		3.4	1516.9	107.2	3.14		
sig94019_16_01	19Jan94	17:46:51.8		3.3	1503.6	107.4	3.18		
sig94019_08_02	19Jan94	11:06:03.0		3.2	1501.5	107.2	2.84		
sig94019_08_00	19Jan94	07:58:32.9		3.1	1508.3	106.9	3.23		
sig94019_16_00	19Jan94	17:02:11.0		3.1	1513.1	106.7	2.45		
sig94032_16_01	1Feb94	18:23:34.9		3.0	1517.2	107.2	2.52		

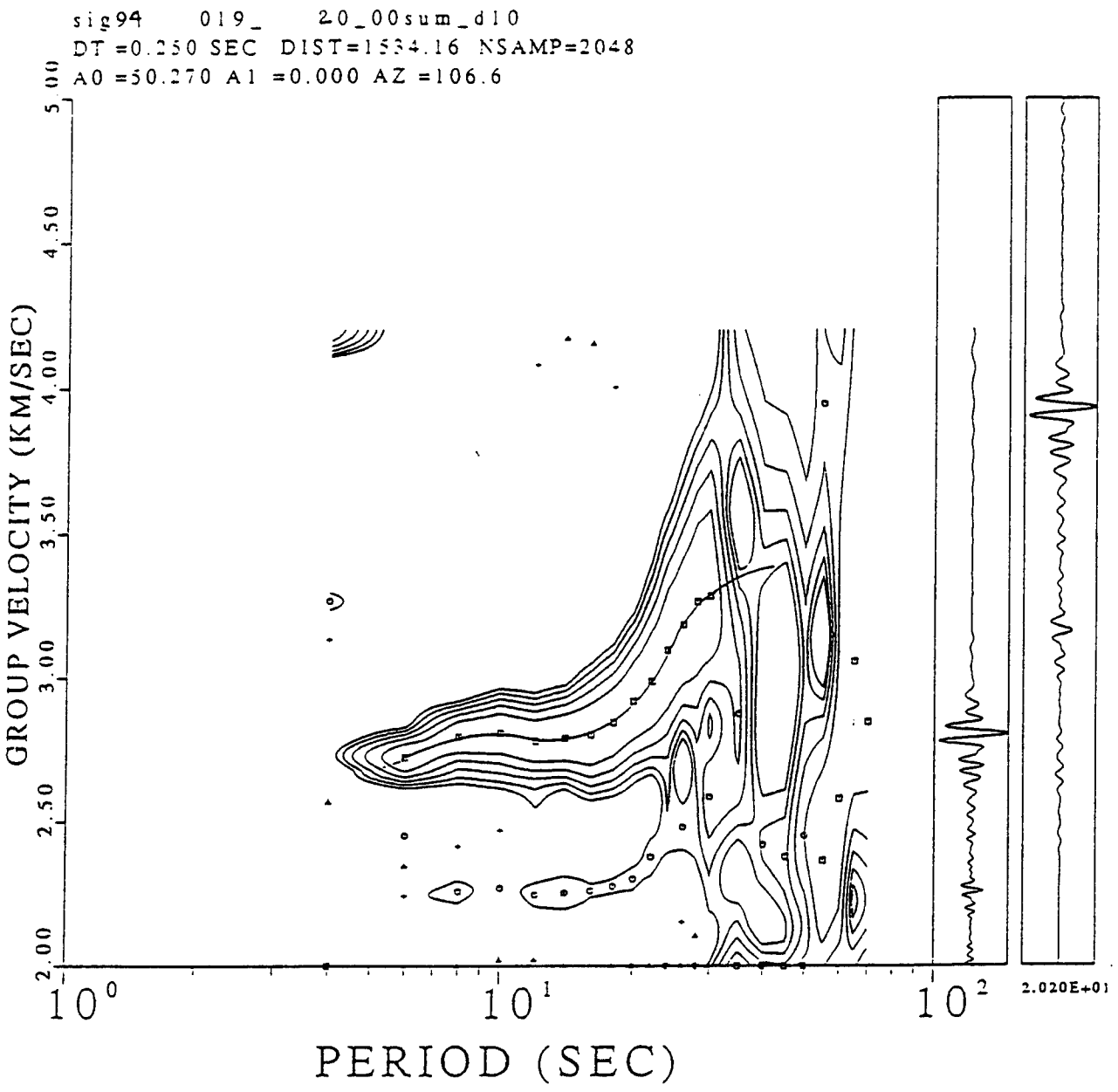

Multiple-filter plot of the reference event sig94019_20_00, m_b=5.0 ML=5.3, showing the fundamental Rayleigh wave group velocity dispersion curve. This event was used to develop the phase-matched filter for the Northridge, California to Lajitas, Texas travel path.

Wave-form to the far right is the input waveform plotted on a linear time scale. The inside waveform is the input signal plotted on a non-linear time scale corresponding to group velocity arrival on the multple-filter plot.

Figure 2. -- Rayleigh Wave Group Dispersion Curve for Northridge Aftershock.

a multiple filter analysis of the reference event using a program supplied by R. Herrmann. The indicated Rayleigh wave dispersion curve was used to design an optimum phase-matched filter (Herrin and Goforth, 1977) which when applied to the reference event produced the results shown in Figure 3. This filter, adjusted for slight differences in epicentral distance, was applied to the low-pass filtered SP sum for 24 events and the low-pass filtered BB Z for 6 events. Spectral Ms at 0.05 Hz was then calculated from the Pseudo Autocorrelation Function (PAF) produced by the phase-matched filters using the formula

$$Ms = \log A/T + \log \Delta \qquad (1)$$

where A is the spectral amplitude and Δ is the epicentral distance in degrees.

Table 1 shows the m_b (Pn) and Ms values for the 25 events which are ordered in decreasing values of ML. It was observed that, on the average, m_b was about 0.3 magnitude units smaller than ML so that the range of magnitudes for the data base was from about m_b 2.7 to 5.0.

Ms values from the SP sum and the BB Z were essentially the same. For both data sources the 20 sec. Rayleigh wave was lost in the noise for events with Ms less than about 3.0 (m_b about 3.5). From Table 1 it is clear that Ms is decreasing faster than m_b with decreasing event size. We can speculate that the value of Ms (20 sec.) for a m_b 3.0 Northridge aftershock would be about 2.5, but neither the SP sum or the BB Z were able to resolve 20 sec. Rayleigh waves at this level.

Unresolved Technical Issues

The 1500 km path from Northridge to Lajitas crosses the Coast Ranges, the Basin and Range Province, and the southward extension of the Rio Grande Rift. This path, roughly analogous to paths across tectonically active areas in the Middle East, causes considerable attenuation of Pn and Rayleigh waves. Thus, the use of the Northridge - Lajitas data set to test the Ms:m_b technique at regional distances constitutes a kind of "worst-case" test of the method.

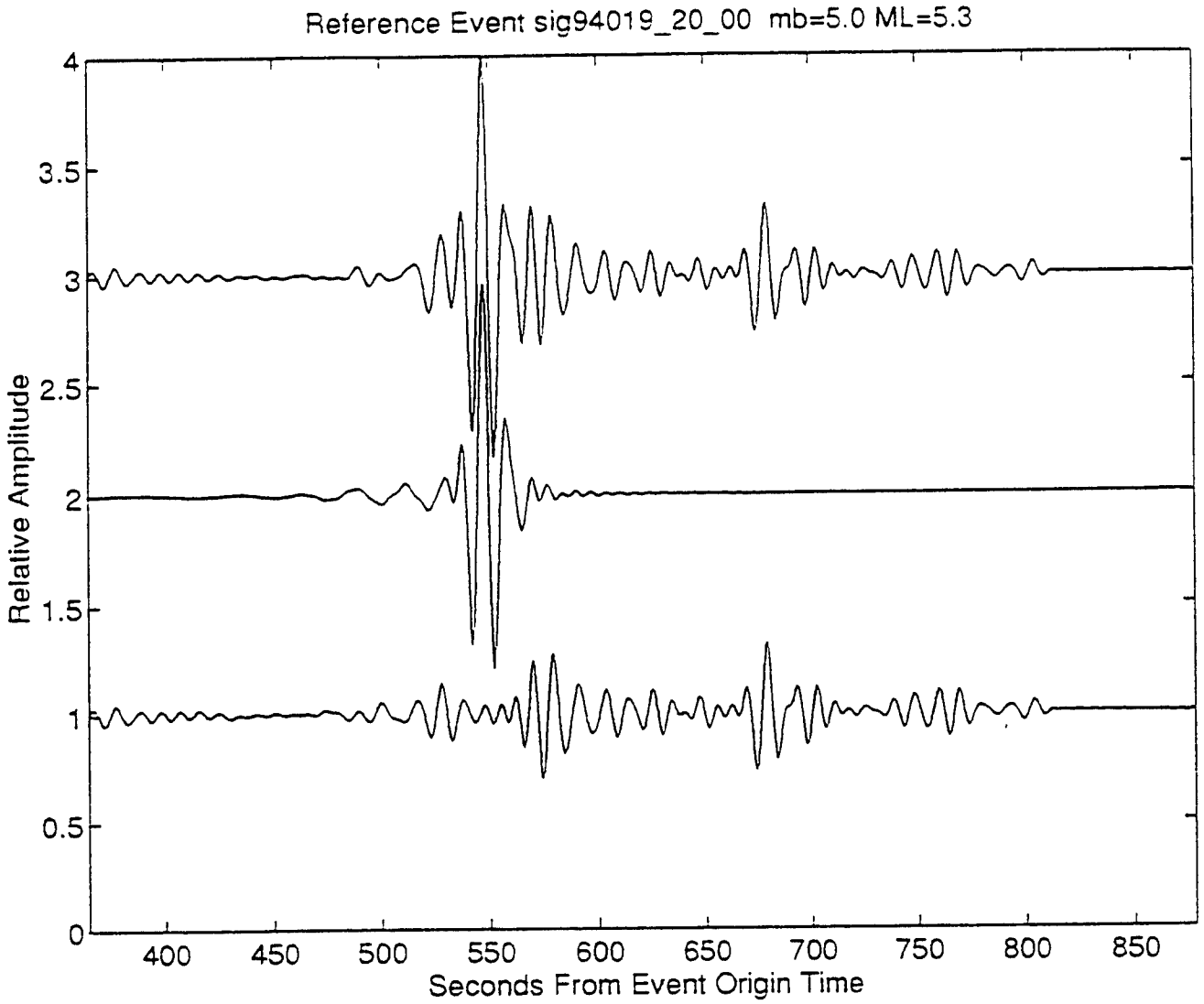

Results of phase-matched filtering of the reference event:

Top trace is the input waveform of reference event sig94019_20_00. The middle trace shows the estimated fundamental Rayleigh wave component of the complex input signal (pseudo autocorrelation function PAF). The bottom trace is a plot of the residual after the estimated fundamental Rayleigh wave (middle trace) is removed from the input signal.

Figure 3. -- Phase Matched Filtering of Northridge Aftershock.

If we are to lower the Ms measurement threshold for this data set to m_b 3.0, we must investigate the nature of the noise floor which now limits the resolution. The SP sum at 20 sec. must have a noise floor at or greater than the instrument noise (10dB above the Low Noise Model) and the BB Z must have a noise floor set by the ambient 20 sec noise at Lajitas (near the Low Noise level) or by non-linear effects caused by the large output voltages at higher frequencies. But the SP sum and BB Z were recorded on different systems and both systems exhibited the same noise floor well above the predicted limits; that is, essentially equivalent to the spectral amplitudes for Ms 3.0 events.

What is the nature of the 20 sec. "noise" which limits the Ms measurements at Lajitas for the Northridge events? How is the "noise" related to ambient background in the absence of regional signals? Can methods be found for increasing the signal-to-noise ratio by about 10 dB in order to obtain Ms measurements for m_b 3.0 events in Southern California?

For Northridge events of m_b about 3.5 the Ms (20 sec.) value has decreased to about 3.0. The use of phase-matched filtering has removed the dispersion effects so that spectral amplitude measurements at or near an Airy phase can be made reliably. Quoting from Davies (1968, SIPRI, p. 62) "When magnitude determination at 20 seconds proves impossible at near distances, Thirlaway considers 12 sec. period waves and applies an appropriate correction...." Would a choice of 12 or 15 sec. period for the Ms measurement result in a significantly lower threshold?

REFERENCES

Davies, David (Rapporteur), 1968, *Seismic Methods for Monitoring Underground Explosions:SIPRI*, Stockholm, 130 p.

Herrin, Eugene, and Tom Goforth ,1977, Phase-matched Filters: Application to the study of Rayleigh waves, *Bull. Seis. Soc. Am.*, **67**, 1250-1275.

Peterson, Jon, 1993, U.S. Geological Survey Open-File Report 92-322.

Rodgers, Peter W., 1992, Frequency limits for seismometers as determined from Signal-to-Noise Ratios: Part 1. The Electromagnetic Seismometer, *Bull. Seis. Soc. Am.*, **82**, 1071-1098.

APPENDIX 4 -- RESEARCH IN REGIONAL EVENT DISCRIMINATION USING Ms:m_b AND AUTOREGRESSIVE MODELING

Eugene Herrin, Valeriu Burlacu, Henry L. Gray, Jack Swanson, Paul Golden and Billie Myers

POSTER SESSION

Sponsored by: Advanced Research Projects Agency, Nuclear Monitoring Office, ARPA Order # A128/16
Issued by: Phillips Laboratory
Contract Number: F19628-93-C-0057

Ms:m_b STUDIES

By 1970, research in the seismic discrimination of explosions and earthquakes had clearly established that the comparison of surface wave magnitude (Ms) and body-wave magnitude (m_b) could be used to classify shallow events. In fact, this method provided the only reliable means for the seismic identification of underground explosions. The Ms:m_b method was shown to be an effective and transportable discriminant for shallow events with m_b greater than 4.75. Further research was carried out including the construction of long-period arrays in an attempt to lower this threshold, but until recently, essentially all data was obtained from stations at teleseismic distances.

Now the construction of regional arrays for monitoring a proposed CTBT has led to considerable interest in reducing the detection threshold for fundamental mode Rayleigh waves using regional signals. Our goal is to identify shallow earthquakes at regional distances with magnitude (m_b) as low as 3.0 using the Ms:m_b method.

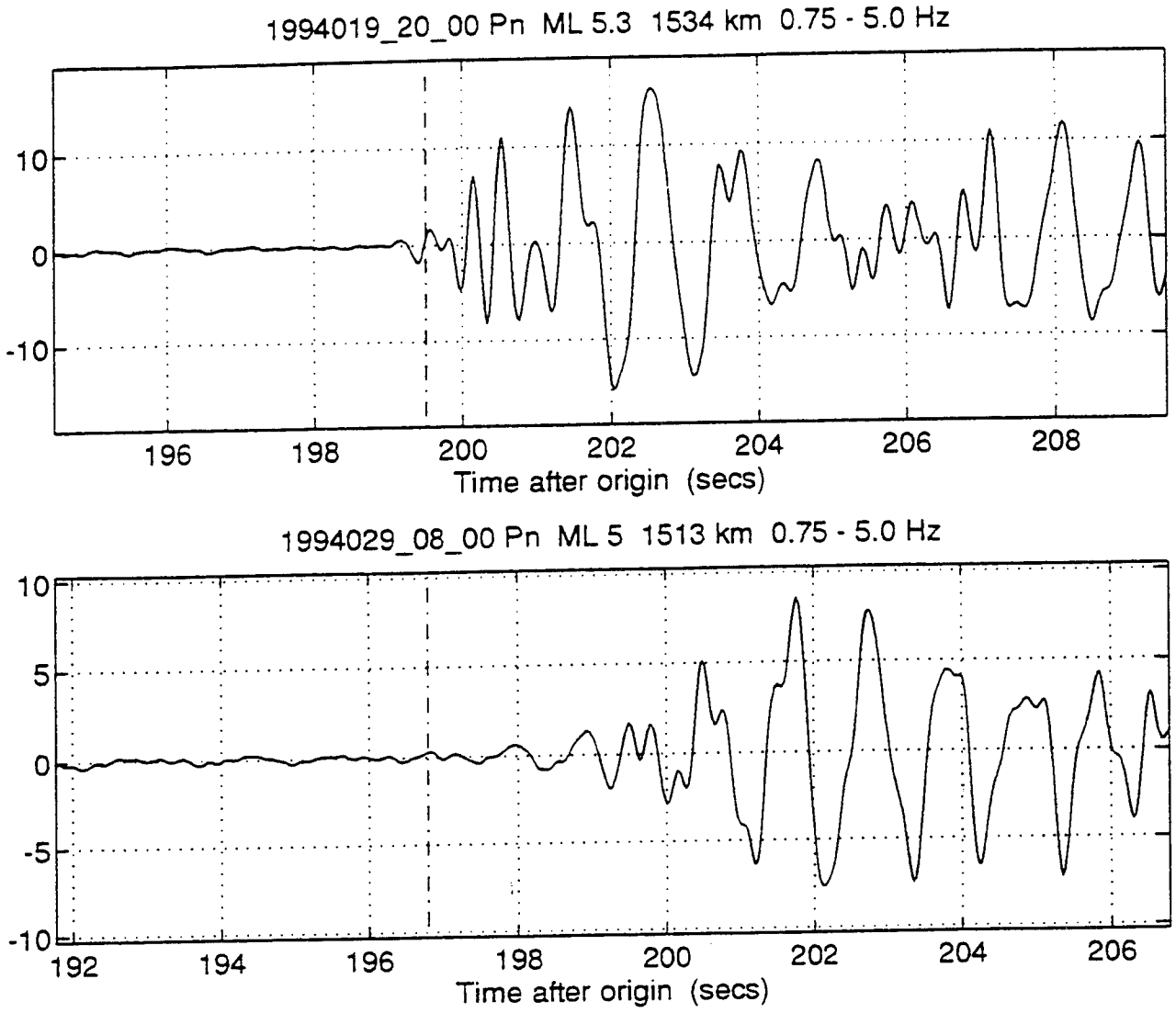

Figure 1. -- Pn arrival 1994019_20_00 and 1994029_08_00

Beam of Pn arrival for two aftershocks of the Northridge earthquake. Beams were formed using time delays determined for the reference event 1994019_20_00. Expected Pn arrival times, based on epicentral distances reported by the USGS and Pn group velocity of 7.69 km/s, are indicated on the plots. The USGS reported m_b 5.0 and no ML for 1994019_20_00 and m_b 4.5 and ML 5.0 for event 1994029_08_00. ML for 1994019_20_00 was estimated as 5.3, based on the relation developed in this study.

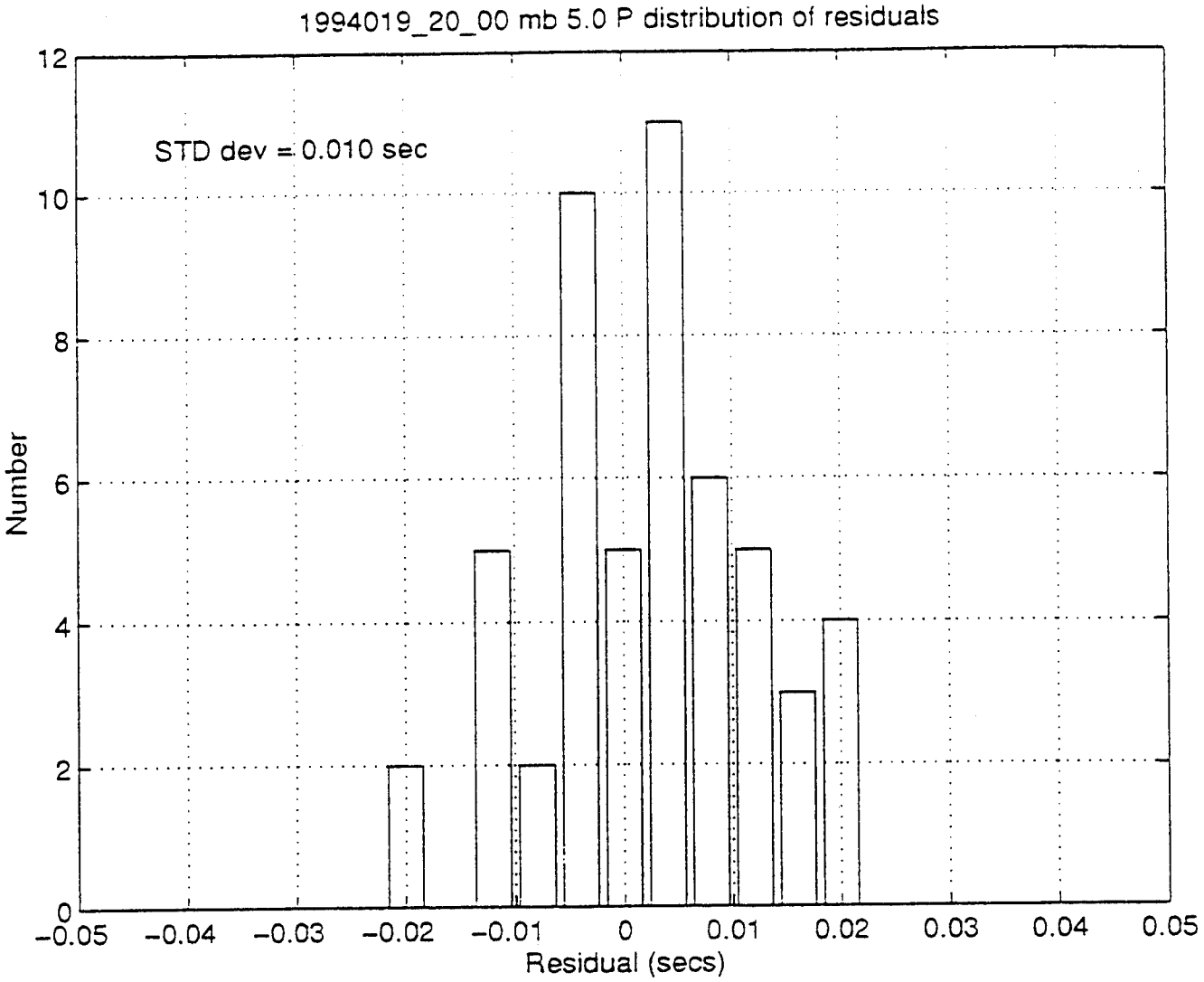

Figure 2. -- Histogram of residuals from least-squares estimate of azimuth and phase velocity of reference event 1994019_20_00 (aftershock of the Northridge earthquake) observed on the Lajitas, TX short period array. Data are combined for residuals obtained using each channel as reference. Estimated azimuth was 291 degrees and estimated phase velocity was 8.46km/s.

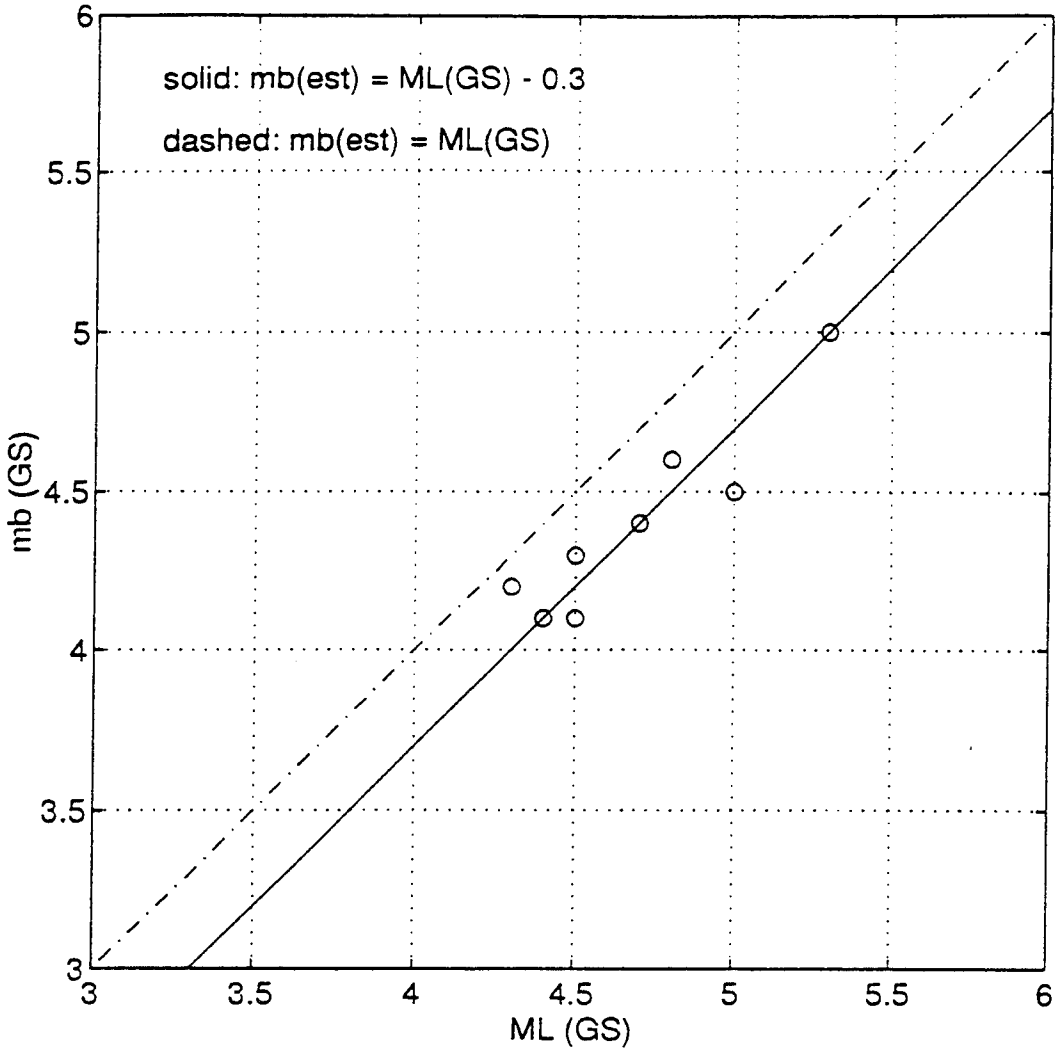

Figure 3. --USGS Magnitudes for Northridge aftershocks

Comparison of body wave and local magnitudes reported by the USGS(GS) for 8 aftershocks of the Northridge earthquake. m_b(GS) averages 0.3 magnitude units smaller than ML(GS).

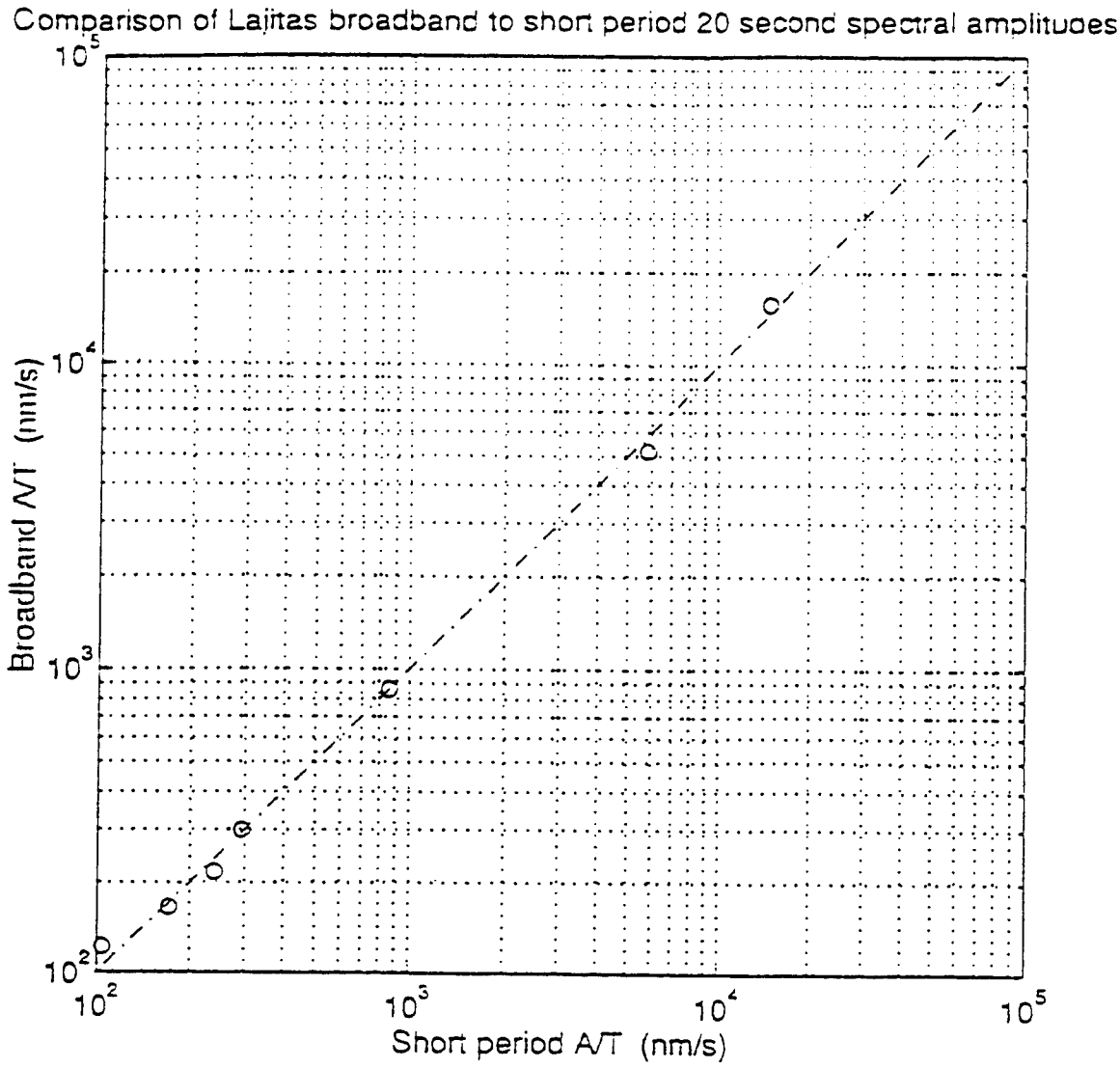

Figure 4. -- Comparison of broadband to short period 20 second spectral amplitudes observed at Lajitas, TX for 7 aftershocks of the Northridge earthquake. Agreement of amplitudes observed on the two systems is good. Gains for the short period system were 132.8 counts/(nm /s) at a period of 1 second and 0.35 counts/(nm/s) at a period of 20 seconds. For the broadband system, gains were 2.0E4 counts/(nm/s) at a period of 1 second and 466.8 counts/(nm/s) at a period of 20 seconds.

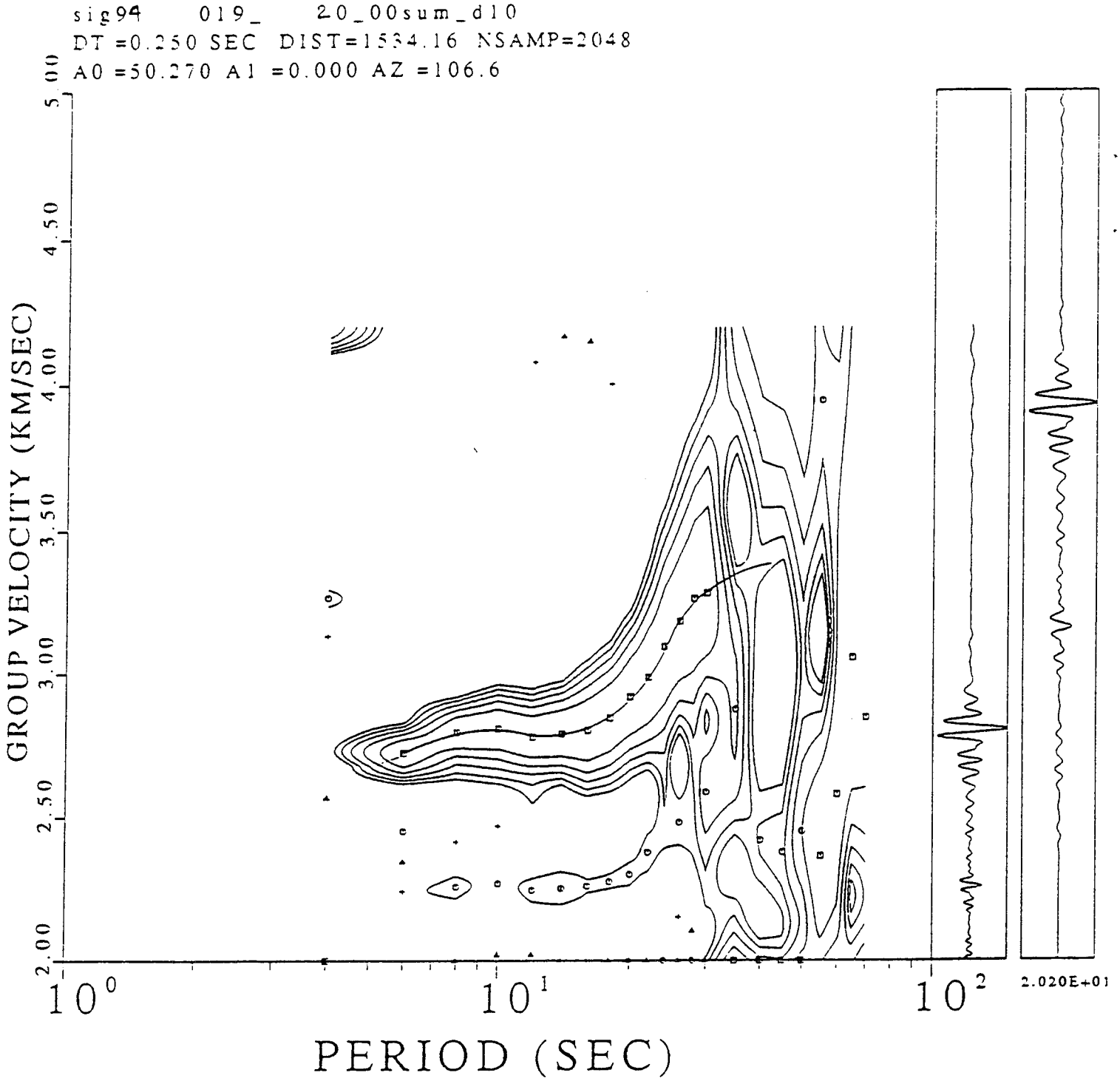

Figure 5. -- Multiple-filter plot of the reference event sig94019_20_00, m_b=5.0 ML=5.3, showing the fundamental Rayleigh wave group velocity dispersion curve. This event was used to develop the phase-matched filter for the Northridge, California to Lajitas, Texas travel path.

Wave-form to the far right is the input waveform plotted on a linear time scale. The inside waveform is the input signal plotted on a non-linear time scale corresponding to group velocity arrival on the multple-filter plot.

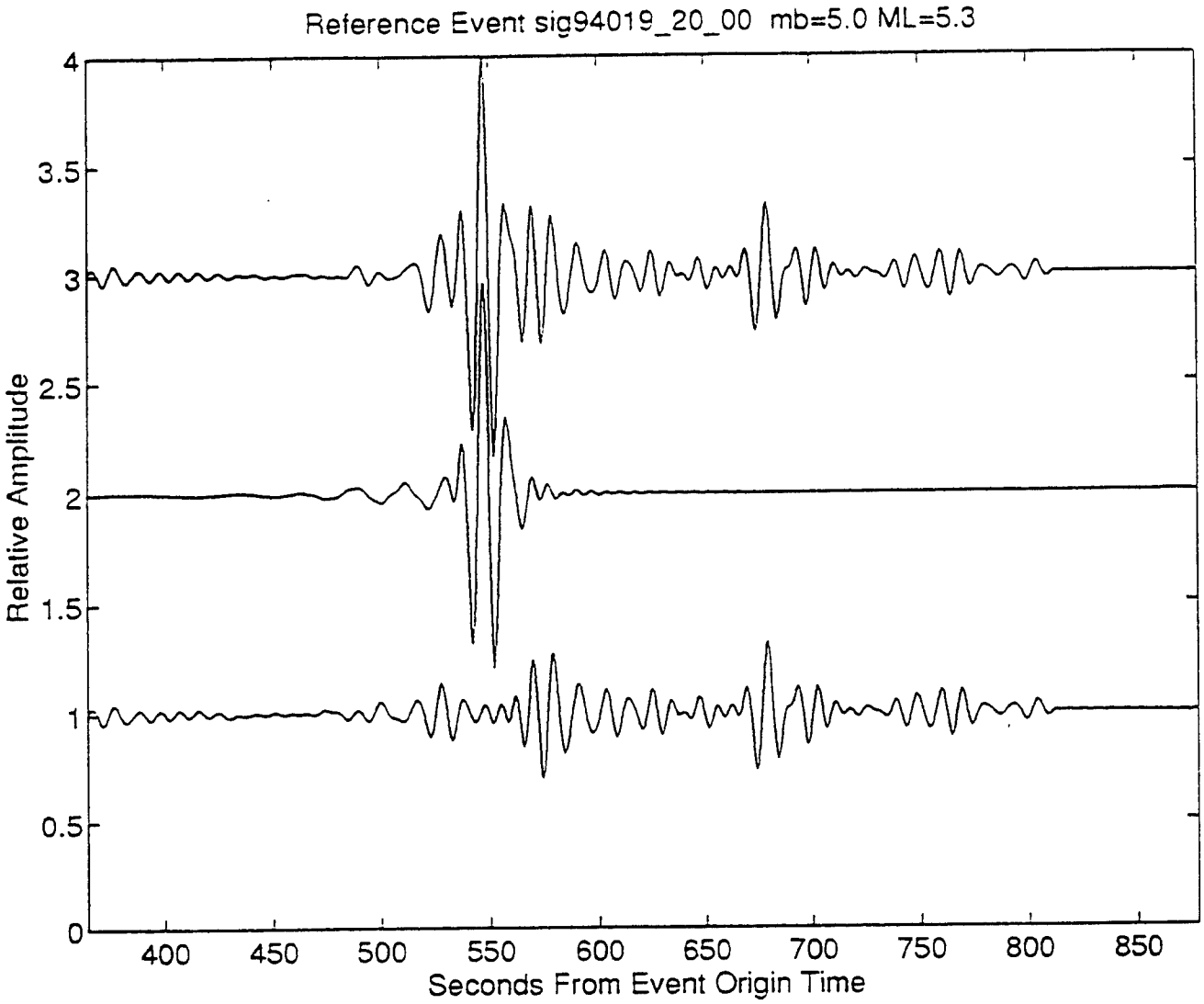

Figure 6. -- Results of phase-matched filtering of the reference event:

Top trace is the input waveform of reference event sig94019_20_00. The middle trace shows the estimated fundamental Rayleigh wave component of the complex input signal (pseudo autocorrelation function PAF). The bottom trace is a plot of the residual after the estimated fundamental Rayleigh wave (middle trace) is removed from the input signal.

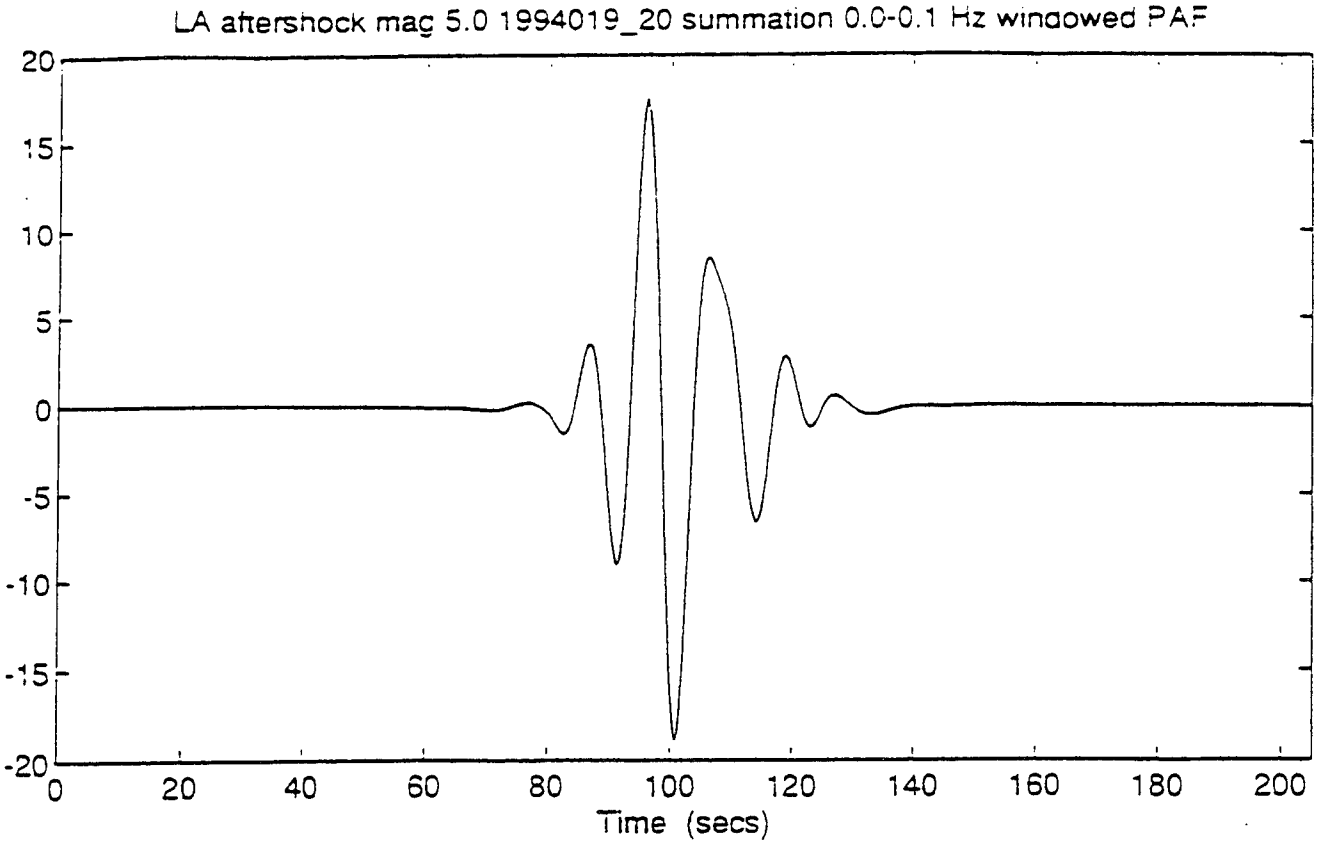

REFERENCE EVENT

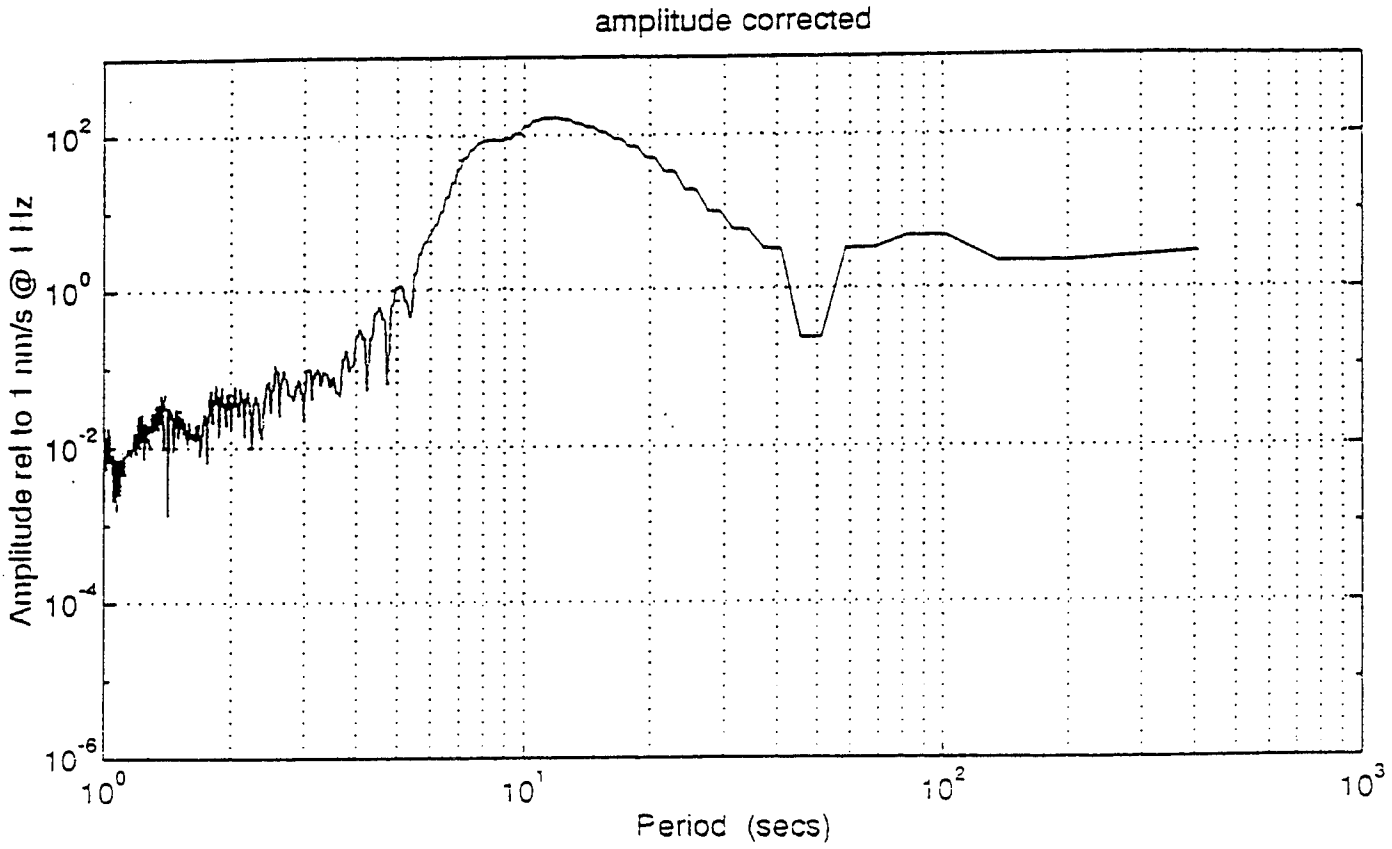

Figure 7. -- Windowed PAF and Spectra of Reference Event

SUMMARY

Ms:m_b FOR NORTHRIDGE AFTERSHOCKS

* sp array and bb surface wave magnitudes are essentially the same.

* USGS m_b is on the average about 0.3 units less than ML for the Northridge aftershocks.

* Ms could be reliably determined for events with m_b about 3.5 and greater at a distance of about 1500 km from Lajitas.

* Lajitas m_b was determined using an array beam with an azimuth of 272° and a horizontal phase velocity of 8.4 km/s.

* Pn arrivals for Lajitas with m_b less than about 3.3 were heavily contaminated by background noise.

AR(3) - Lg METHOD

Spectral content of regional phases (Pn, Pg, Lg) has been shown by Murphy and Bennett to be important in the design of algorithms for discrimination between earthquakes and explosions. Techniques using spectral ratios have been applied to data in the Western U.S. and in Europe with reasonable success, but the transportability of the methods has not been satisfactorily established. Wüster used ARMA (Auto-Regressive, Moving Average) spectral estimates in the development of discriminants. The discriminant we studied is based on autoregressive modeling of the Lg phase. The initial data is from Grant/Coyne/Ryall CSS Ground Truth Data Base recorded at GERESS (16 Hz bandwidth). Figure 1 is a location map of the GERESS-Vogtland area. The data consists of explosions and earthquakes in the Vogtland area (see Table 1 of Appendix 2 on page 23 of this report).

The magnitude range is 1.93 - 2.15 for the quarry blasts and 1.4 - 2.37 for earthquakes. The origin times were calculated assuming Jeffreys-Bullen travel time curves. From the waveforms, those recorded by GEC2 (the most reliable station in the GERESS array) were used.

AR (ALL POLE) PROCESS

$$x(n)=-\sum_{k=1}^{p} a(k)x(n-k)+u(n)$$

p is the order of the process.

a(k) are the coefficients, generally complex.

u(n) is the driving process, here assumed to be white noise.

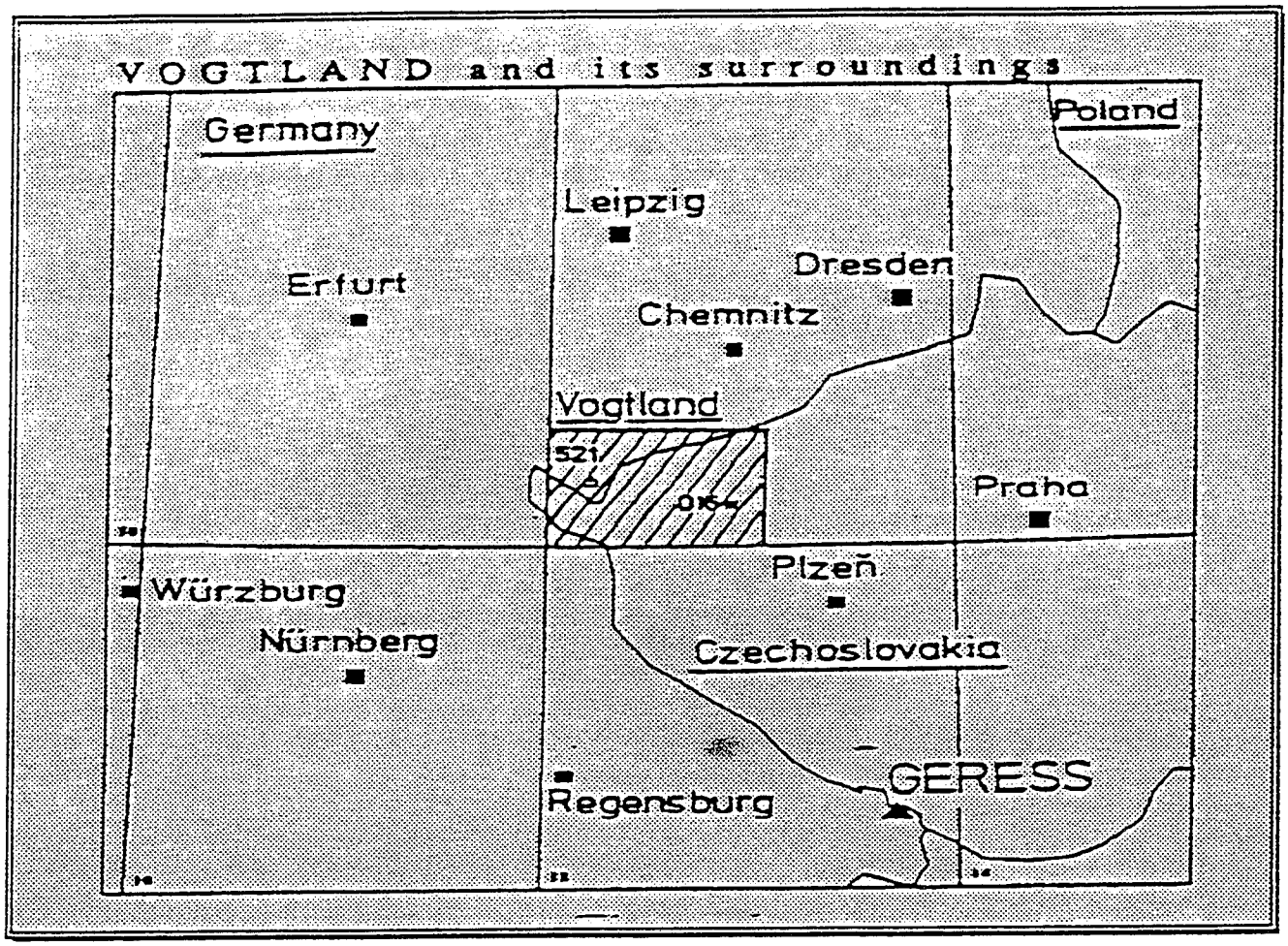

Figure 1. The Vogtland area and the location of the GERESS array(after Wüster, 1993)

Figure 8. -- Location Map of GERESS-Vogtland Area

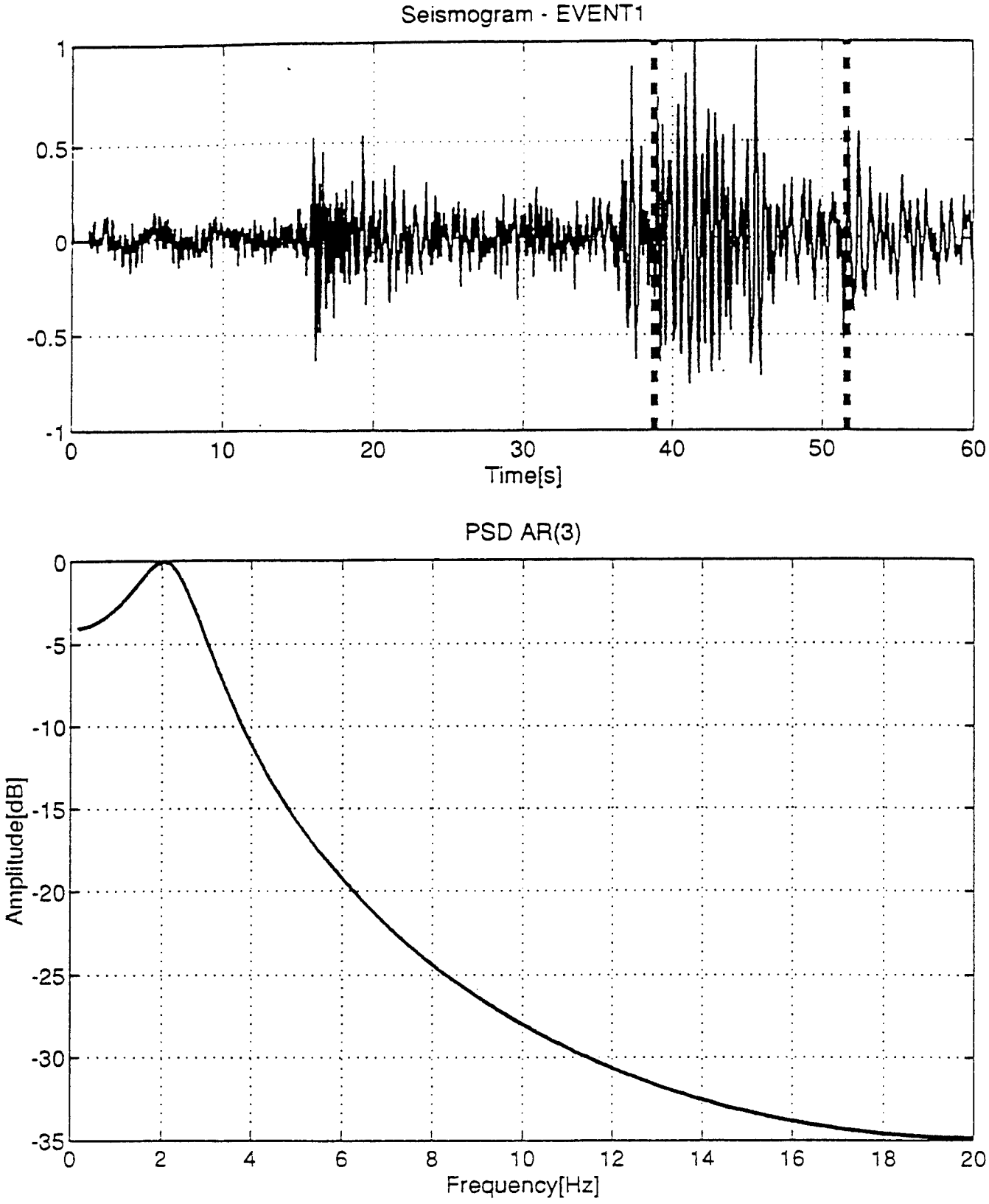

Figure 9. -- Seismogram and Spectra for Quarry Blast (EVENT 1)

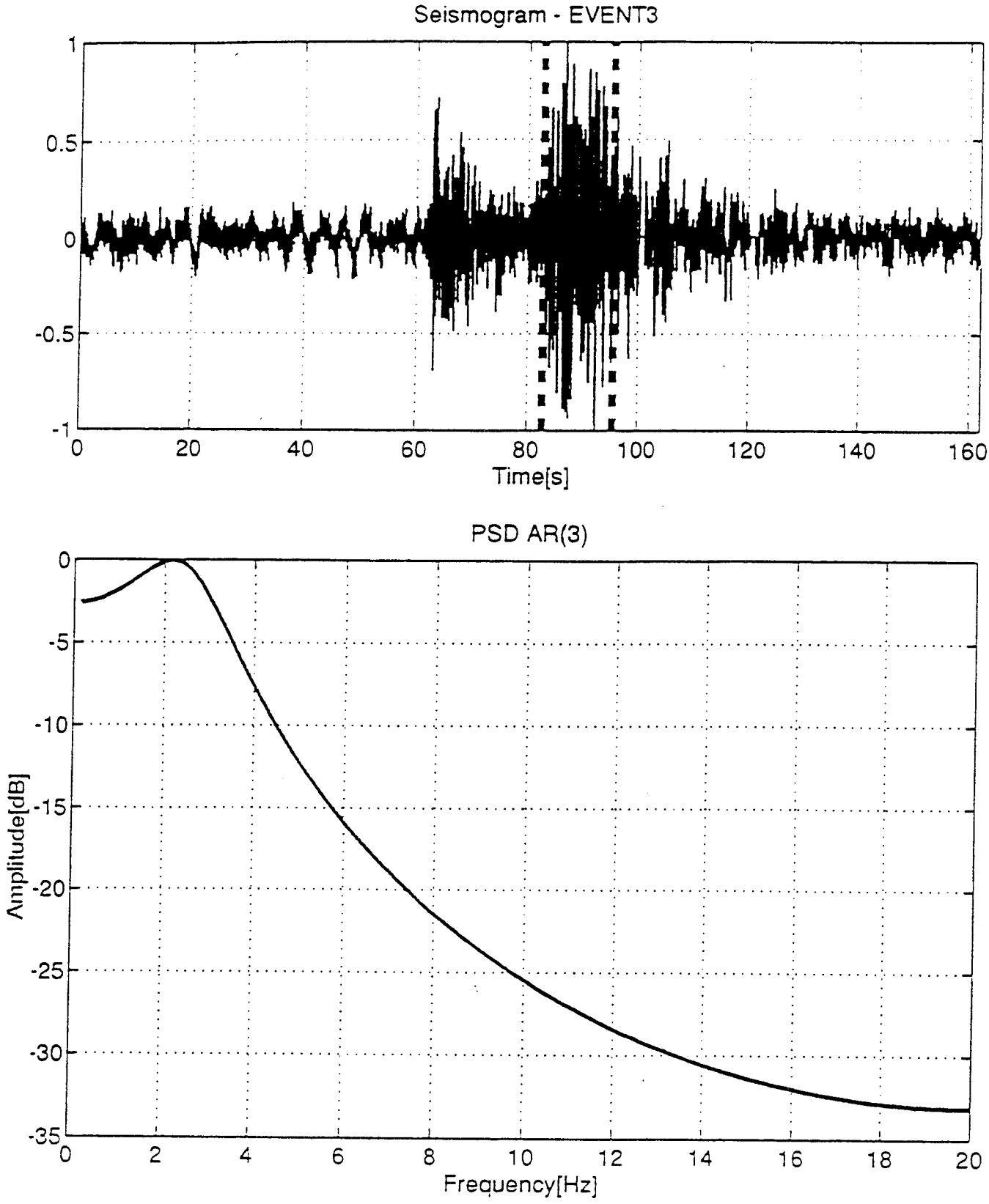

Figure 10. -- Seismogram and Spectra for Quarry Blast (EVENT 3)

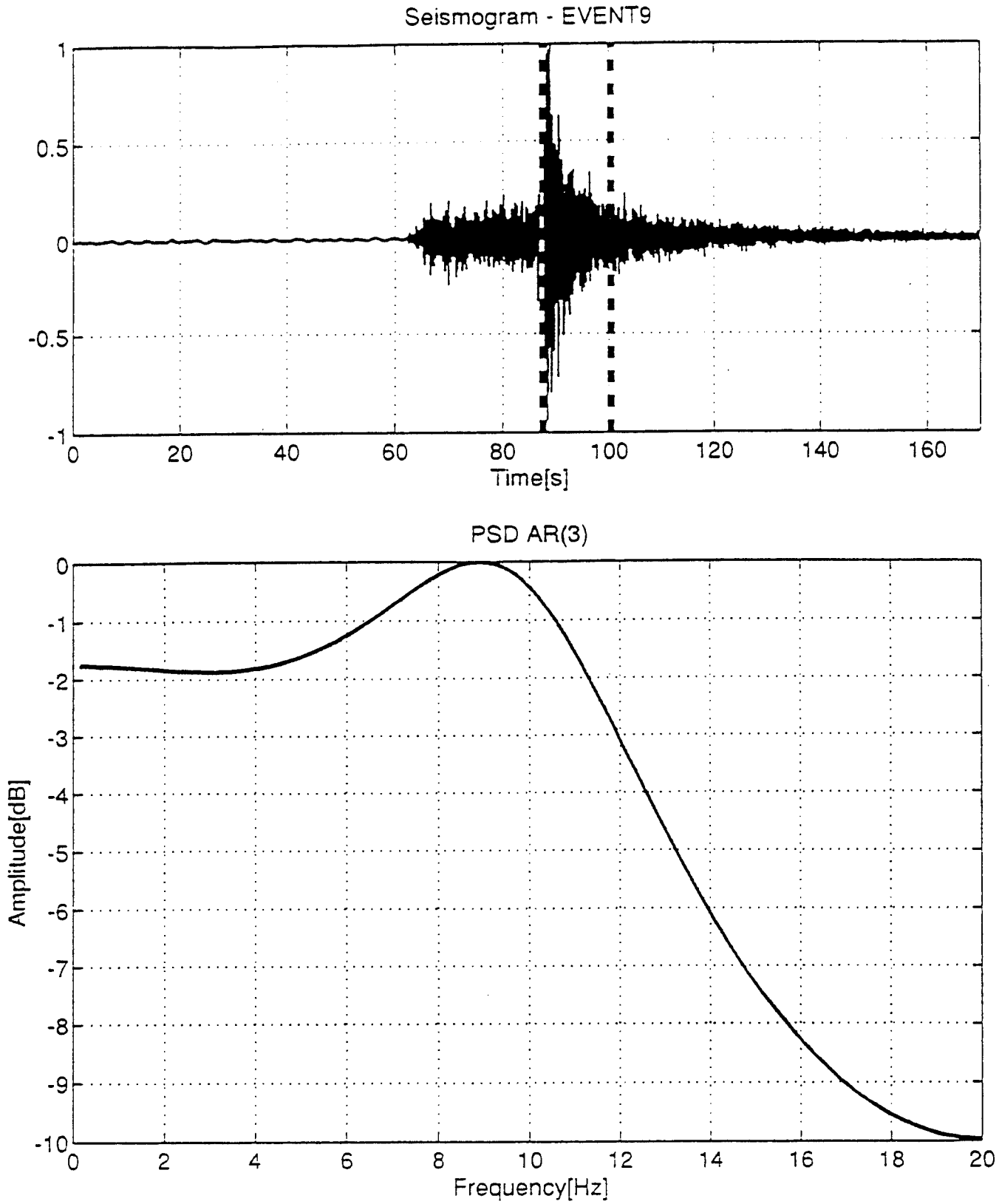

Figure 11. -- Seismogram and Spectra for Earthquake (EVENT 6)

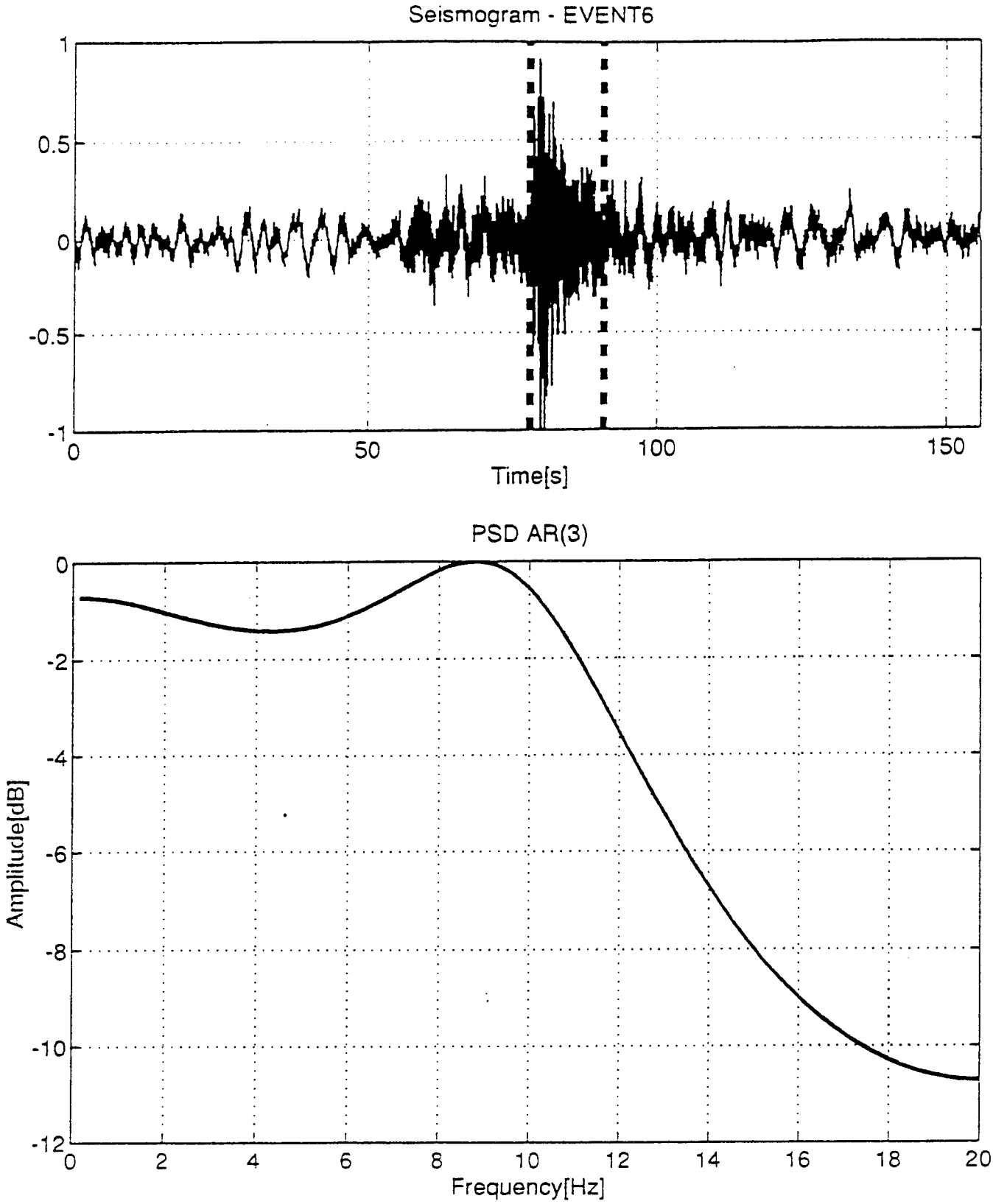

Figure 12. -- Seismogram and Spectra for Earthquake (EVENT 9)

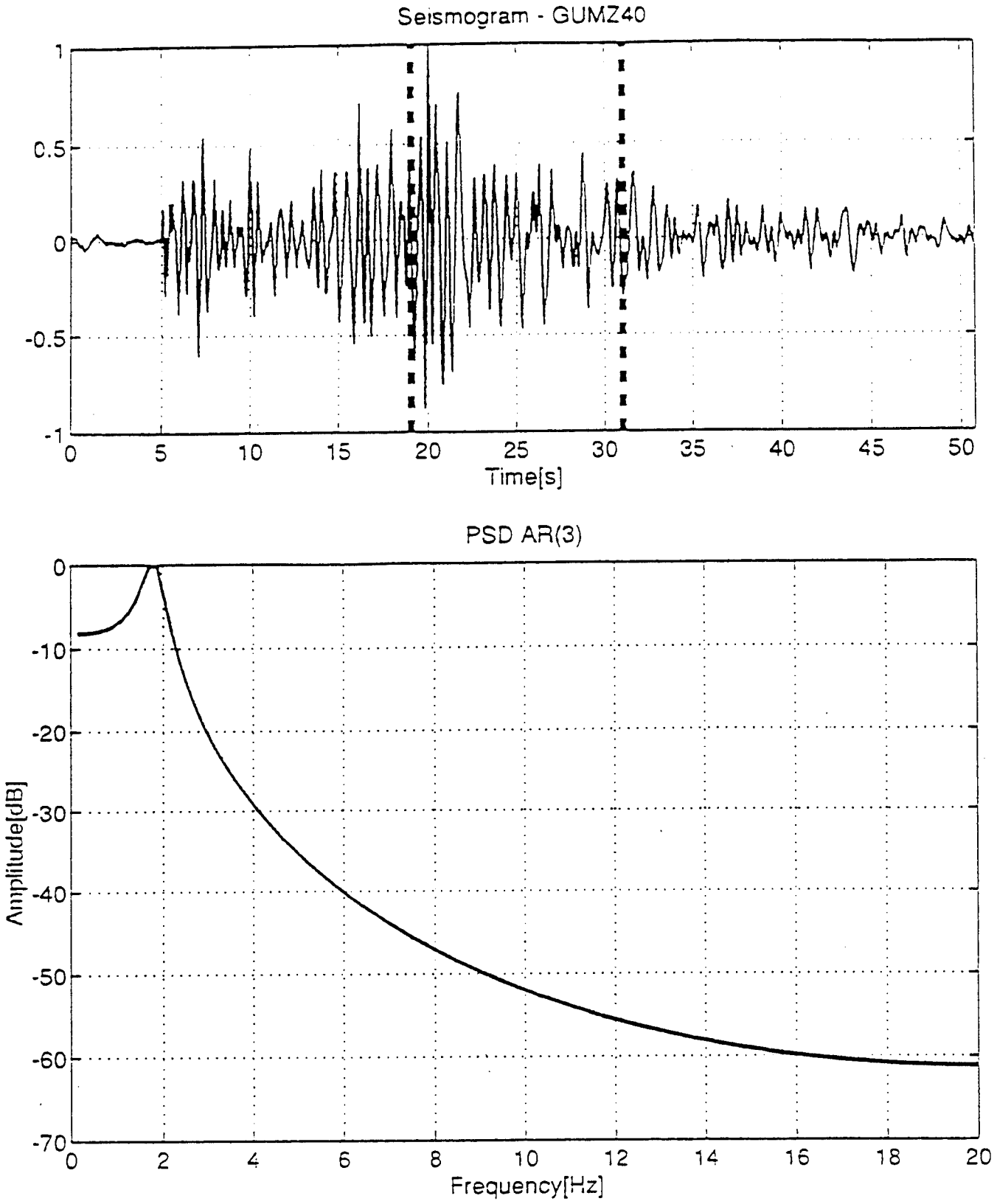

Figure 13. -- Seismogram and Spectra for Mine Blast from Southern Russia

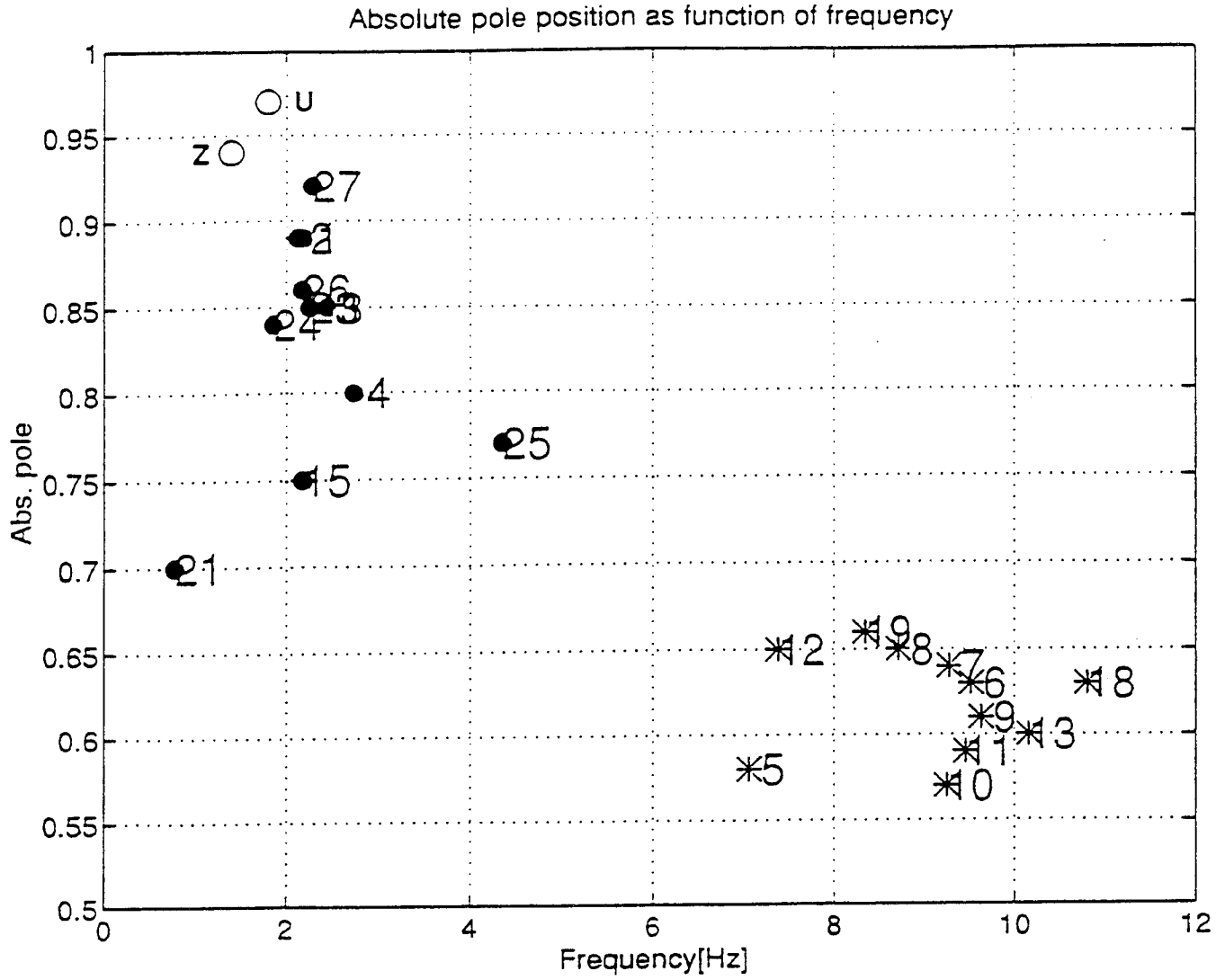

Figure 14. -- The AR(3) model has one real pole and two paired complex poles. This figure shows the three reciprocal poles in the complex plane. Angular frequency is from zero to $\pm \pi$, the latter being the folding frequency. The real pole can only be at one of these two frequencies. Only the complex pole for positive frequency need be considered in the interpretation of the model. For AR process to be stable, the poles must all lie outside the unit circle, therefore the reciprocal poles must lie between the origin and the unit circle. In practice, their position cannot be zero or one. The nearer the reciprocal pole to the unit circle, the "stronger" it appears in the AR spectrum.

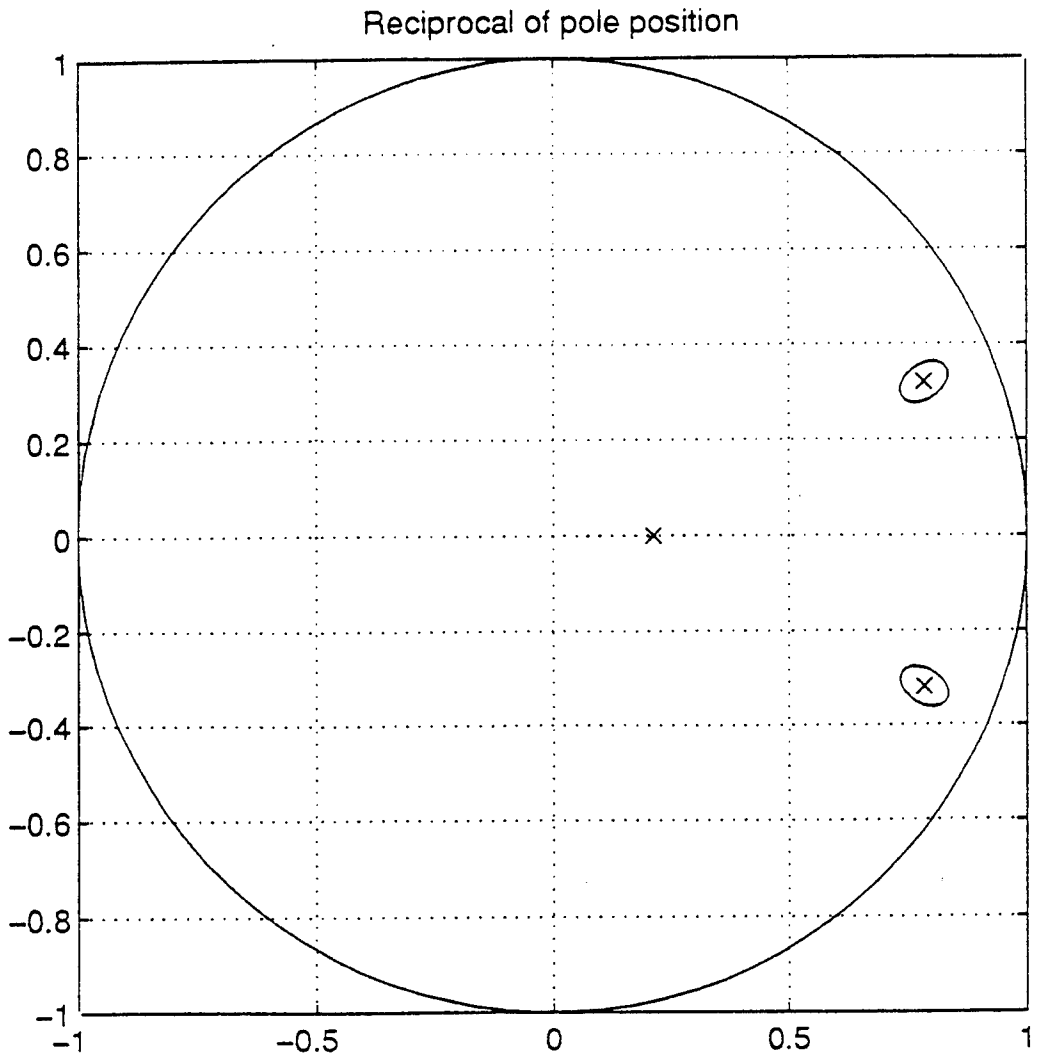

Figure 15. -- Reciprocal pole position vs frequency for the analyzed events. Solid circles are explosions and stars are earthquakes. The two open circles represent surface and buried explosions at the Tyrnyaus mine in the Caucasus Mountains of Southern Russia recorded at station GUM. This figure shows a clear separation of explosions and earthquakes with the latter having broad AR(3) spectra with "weak" poles above 6 Hz while the explosions all show much "stronger" poles at frequencies less than 5 Hz.

SUMMARY

AR(3) - Lg METHOD

* The method is simple and robust.

* Because spectral amplitudes or spectral ratios are not used, extensive calibrations are not required.

* Only the vertical record of Lg is needed. The method does not require good signal-to-noise ratio for the body wave arrivals.

* The method has provided complete discrimination for all events we have analyzed which were recorded with 16 Hz bandwidth and for which the source type is known.

APPENDIX 5. -- INSTALLATION OF POSTHOLE 54000 SEISMOMETER

Eugene Herrin

1. Hole was prepared using the technique described for GS-13 installations. Casing IDE nominal 8 in. Depth nominal 20 ft.

2. 54,000 PH package was equipped with flat nose plate and standard armored cable.

3. Casing was marked N-S. 54,000 PH was marked N-S.

4. Very fine, clean sand (sand blasting material) was introduced into the hole to a thickness of 2 to 4 inches. Sand was introduced through a plastic pipe 24 feet long with a funnel on top in order to minimize dust in hole.

5. With the masses locked the 54,000 PH package was lowered into hole, positioned approximately in center of hole and rotated so N-S sensor was lined up with N-S direction marked on casing.

6. Sand was carefully introduced into hole using plastic pipe until sand level was about 1/2 way up on the 54,000 PH package.

7. A steel pipe with an eccentric on the lower end and a horizontal rod on the upper end was used to tilt the upper end of the 54,000 PH package until the level bubble on top of the package was centered. Bubble was observed using a Nikon spotting scope on a tripod and a 500,000 CP battery powered hand-lamp.

8. The 54,000 PH control box was connected to the up-hole end of the armored cable. Power was provided to the control box (110 vac) and the three masses were unlocked.

9. The mass position (DC) output voltage was read and it was determined that the mass was captured by the feed-back process.

10. The signal output of the vertical component was observed to determine that the Z-component was operational.

11. Two meters were used to read the mass position (MP) output voltage of the N-S and E-W components. In general, both voltages would be full-scale (power supply voltage about $\pm$ 13 vdc) indicating that the masses were not captured. Polarity was N and E positive.

12. The pipe-tool was used to move the top of the instrument along the N-S axis in the required direction (toward zero MP voltage). A steady pressure was required to be applied to the side of the upper end of the package and held until the sand could flow to accommodate a tilt in the package. The process was repeated until the N-S mass was captured (MP output less than $\pm$ 12 vdc).

13. This process can be time consuming and frustrating. A great deal of time and pressure was required to move the top of the package only a very small fraction of an inch.

14. When the N-S was captured the E-W MP voltage was read. Let us assume an E-W value of +13 volts so that the top would need to be moved to the west. Also assume a MP output of + 11 volts indicating a tilt to the north.

15. The pipe tool was repositioned to push the top of the package to the southwest. Pressure was applied until the N-S MP output was about -11 vdc.

16. The tool was repositioned to push the top of the package to the northwest until the N-S MP was about + 11 vdc.

17. This process was repeated until the E-W mass was captured. A near capture condition is indicated by the MP output changing rapidly as pressure is applied to the top of the hole and then slowly drifting back to the stop after pressure is released.

18. Once all masses were captured the N-S and E-W tilts could be carefully trimmed until MP output on both horizontal channels were $\pm$ a couple of volts or less.

19. The signal outputs were observed to insure that all the components were measuring seismic activity.

20. The hole and cable were put into the final operational configuration. If desired, more sand can be introduced around the 54,000 PH package for stability, but after the experience of trying to tilt the package using the pipe tool, you will probably conclude that no more sand is needed.

Prof. Thomas Ahrens
Seismological Lab, 252-21
Division of Geological & Planetary Sciences
California Institute of Technology
Pasadena, CA 91125

Prof. Keiiti Aki
Center for Earth Sciences
University of Southern California
University Park
Los Angeles, CA 90089-0741

Prof. Shelton Alexander
Geosciences Department
403 Deike Building
The Pennsylvania State University
University Park, PA 16802

Dr. Thomas C. Bache, Jr.
Science Applications Int'l Corp.
10260 Campus Point Drive
San Diego, CA 92121 (2 copies)

Prof. Muawia Barazangi
Cornell University
Institute for the Study of the Continent
3126 SNEE Hall
Ithaca, NY 14853

Dr. Douglas R. Baumgardt
ENSCO, Inc
5400 Port Royal Road
Springfield, VA 22151-2388

Dr. T.J. Bennett
S-CUBED
A Division of Maxwell Laboratories
11800 Sunrise Valley Drive, Suite 1212
Reston, VA 22091

Dr. Robert Blandford
AFTAC/TT, Center for Seismic Studies
1300 North 17th Street
Suite 1450
Arlington, VA 22209-2308

Dr. Steven Bratt
ARPA/NMRO
3701 North Fairfax Drive
Arlington, VA 22203-1714

Dale Breding
U.S. Department of Energy
Recipient, IS-20, GA-033
Office of Arms Control
Washington, DC 20585

Dr. Jerry Carter
Center for Seismic Studies
1300 North 17th Street
Suite 1450
Arlington, VA 22209-2308

Mr Robert Cockerham
Arms Control & Disarmament Agency
320 21st Street North West
Room 5741
Washington, DC 20451,

Dr. Zoltan Der
ENSCO, Inc.
5400 Port Royal Road
Springfield, VA 22151-2388

Dr. Stanley K. Dickinson
AFOSR/NM
110 Duncan Avenue
Suite B115
Bolling AFB, DC

Dr Petr Firbas
Institute of Physics of the Earth
Masaryk University Brno
Jecna 29a
612 46 Brno, Czech Republic

Dr. Mark D. Fisk
Mission Research Corporation
735 State Street
P.O. Drawer 719
Santa Barbara, CA 93102

Dr. Cliff Frolich
Institute of Geophysics
8701 North Mopac
Austin, TX 78759

Dr. Holly Given
IGPP, A-025
Scripps Institute of Oceanography
University of California, San Diego
La Jolla, CA 92093

Dr. Jeffrey W. Given
SAIC
10260 Campus Point Drive
San Diego, CA 92121

Dr. Dale Glover
Defense Intelligence Agency
ATTN: ODT-1B
Washington, DC 20301

Dan N. Hagedon
Pacific Northwest Laboratories
Battelle Boulevard
Richland, WA 99352

Dr. James Hannon
Lawrence Livermore National Laboratory
P.O. Box 808, L-205
Livermore, CA 94550

Dr. Roger Hansen
University of Colorado, JSPC
Campus Box 583
Boulder, CO 80309

Prof. David G. Harkrider
Division of Geological & Planetary Sciences
California Institute of Technology
Pasadena, CA 91125

Prof. Danny Harvey
University of Colorado, JSPC
Campus Box 583
Boulder, CO 80309

Prof. Donald V. Helmberger
Division of Geological & Planetary Sciences
California Institute of Technology
Pasadena, CA 91125

Prof. Eugene Herrin
Geophysical Laboratory
Southern Methodist University
Dallas, TX 75275

Prof. Robert B. Herrmann
Department of Earth & Atmospheric Sciences
St. Louis University
St. Louis, MO 63156

Prof. Lane R. Johnson
Seismographic Station
University of California
Berkeley, CA 94720

Prof. Thomas H. Jordan
Department of Earth, Atmospheric &
Planetary Sciences
Massachusetts Institute of Technology
Cambridge, MA 02139

Robert C. Kemerait
ENSCO, Inc.
445 Pineda Court
Melbourne, FL 32940

U.S. Dept of Energy
Max Koontz, NN-20, GA-033
Office of Research and Develop.
1000 Independence Avenue
Washington, DC 20585

Dr. Richard LaCoss
MIT Lincoln Laboratory, M-200B
P.O. Box 73
Lexington, MA 02173-0073

Prof. Charles A. Langston
Geosciences Department
403 Deike Building
The Pennsylvania State University
University Park, PA 16802

Jim Lawson, Chief Geophysicist
Oklahoma Geological Survey
Oklahoma Geophysical Observatory
P.O. Box 8
Leonard, OK 74043-0008

Prof. Thorne Lay
Institute of Tectonics
Earth Science Board
University of California, Santa Cruz
Santa Cruz, CA 95064

Dr. William Leith
U.S. Geological Survey
Mail Stop 928
Reston, VA 22092

Mr. James F. Lewkowicz
Phillips Laboratory/GPE
29 Randolph Road
Hanscom AFB, MA 01731-3010(2 copies)

Dr. Gary McCartor
Department of Physics
Southern Methodist University
Dallas, TX 75275

Prof. Thomas V. McEvilly
Seismographic Station
University of California
Berkeley, CA 94720

Dr. Keith L. McLaughlin
S-CUBED
A Division of Maxwell Laboratory
P.O. Box 1620
La Jolla, CA 92038-1620

Prof. Bernard Minster
IGPP, A-025
Scripps Institute of Oceanography
University of California, San Diego
La Jolla, CA 92093

Prof. Brian J. Mitchell
Department of Earth & Atmospheric Sciences
St. Louis University
St. Louis, MO 63156

Mr. Jack Murphy
S-CUBED
A Division of Maxwell Laboratory
11800 Sunrise Valley Drive, Suite 1212
Reston, VA 22091 (2 Copies)

Dr. Keith K. Nakanishi
Lawrence Livermore National Laboratory
L-025
P.O. Box 808
Livermore, CA 94550

Prof. John A. Orcutt
IGPP, A-025
Scripps Institute of Oceanography
University of California, San Diego
La Jolla, CA 92093

Dr. Howard Patton
Lawrence Livermore National Laboratory
L-025
P.O. Box 808
Livermore, CA 94550

Dr. Frank Pilotte
HQ AFTAC/TT
1030 South Highway A1A
Patrick AFB, FL 32925-3002

Dr. Jay J. Pulli
Radix Systems, Inc.
201 Perry Parkway
Gaithersburg, MD 20877

Prof. Paul G. Richards
Lamont-Doherty Earth Observatory
of Columbia University
Palisades, NY 10964

Mr. Wilmer Rivers
Multimax Inc.
1441 McCormick Drive
Landover, MD 20785

Dr. Alan S. Ryall, Jr.
Lawrence Livermore National Laboratory
L-025
P.O. Box 808
Livermore, CA 94550

Dr.Chandan K. Saikia
Woodward Clyde- Consultants
566 El Dorado Street
Pasadena, CA 91101

Mr. Dogan Seber
Cornell University
Inst. for the Study of the Continent
3130 SNEE Hall
Ithaca, NY 14853-1504

Secretary of the Air Force
(SAFRD)
Washington, DC 20330

Office of the Secretary of Defense
DDR&E
Washington, DC 20330

Thomas J. Sereno, Jr.
Science Application Int'l Corp.
10260 Campus Point Drive
San Diego, CA 92121

Dr. Michael Shore
Defense Nuclear Agency/SPSS
6801 Telegraph Road
Alexandria, VA 22310

Prof. David G. Simpson
IRIS, Inc.
1616 North Fort Myer Drive
Suite 1050
Arlington, VA 22209

Dr. Jeffrey Stevens
S-CUBED
A Division of Maxwell Laboratory
P.O. Box 1620
La Jolla, CA 92038-1620

Prof. Brian Stump
Los Alamos National Laboratory
EES-3
Mail Stop C-335
Los Alamos, NM 87545

Prof. Tuncay Taymaz
Istanbul Technical University
Dept. of Geophysical Engineering
Mining Faculty
Maslak-80626, Istanbul Turkey

Prof. M. Nafi Toksoz
Earth Resources Lab
Massachusetts Institute of Technology
42 Carleton Street
Cambridge, MA 02142

Dr. Larry Turnbull
CIA-OSWR/NED
Washington, DC 20505

Dr. Karl Veith
EG&G
5211 Auth Road
Suite 240
Suitland, MD 20746

Prof. Terry C. Wallace
Department of Geosciences
Building #77
University of Arizona
Tuscon, AZ 85721

Dr. William Wortman
Mission Research Corporation
8560 Cinderbed Road
Suite 700
Newington, VA 22122

ARPA, OASB/Library
3701 North Fairfax Drive
Arlington, VA 22203-1714

HQ DNA
ATTN: Technical Library
Washington, DC 20305

Defense Technical Information Center
Cameron Station
Alexandria, VA 22314 (2 Copies)

TACTEC
Battelle Memorial Institute
505 King Avenue
Columbus, OH 43201 (Final Report)

Phillips Laboratory
ATTN: GPE
29 Randolph Road
Hanscom AFB, MA 01731-3010

Phillips Laboratory
ATTN: TSML
5 Wright Street
Hanscom AFB, MA 01731-3004

Phillips Laboratory
ATTN: PL/SUL
3550 Aberdeen Ave SE
Kirtland, NM 87117-5776 (2 copies)

Dr. Michel Campillo
Observatoire de Grenoble
I.R.I.G.M.-B.P. 53
38041 Grenoble, FRANCE

Dr. Kin Yip Chun
Geophysics Division
Physics Department
University of Toronto
Ontario, CANADA

Prof. Hans-Peter Harjes
Institute for Geophysic
Ruhr University/Bochum
P.O. Box 102148
4630 Bochum 1, GERMANY

Prof. Eystein Husebye
NTNF/NORSAR
P.O. Box 51
N-2007 Kjeller, NORWAY

David Jepsen
Acting Head, Nuclear Monitoring Section
Bureau of Mineral Resources
Geology and Geophysics
G.P.O. Box 378, Canberra, AUSTRALIA

Ms. Eva Johannisson
Senior Research Officer
FOA
S-172 90 Sundbyberg, SWEDEN

Dr. Peter Marshall
Procurement Executive
Ministry of Defense
Blacknest, Brimpton
Reading FG7-FRS, UNITED KINGDOM

Dr. Bernard Massinon, Dr. Pierre Mechler
Societe Radiomana
27 rue Claude Bernard
75005 Paris, FRANCE (2 Copies)

Dr. Svein Mykkeltveit
NTNT/NORSAR
P.O. Box 51
N-2007 Kjeller, NORWAY (3 Copies)

Dr. Jorg Schlittenhardt
Federal Institute for Geosciences & Nat'l Res.
Postfach 510153
D-30631 Hannover , GERMANY

Dr. Johannes Schweitzer
Institute of Geophysics
Ruhr University/Bochum
P.O. Box 1102148
4360 Bochum 1, GERMANY

Trust & Verify
VERTIC
Carrara House
20 Embankment Place
London WC2N 6NN, ENGLAND